Towards a catalog of pome tree architecture genes: the draft 'd'Anjou' genome (*Pyrus communis* L.)

Innovating towards architecture genes in pear

Huiting Zhang [1, 2], Eric K. Wafula[3], Jon Eilers[1], Alex E. Harkess[4,5], Paula E. Ralph[3], Prakash Raj Timilsena[3], Claude W. dePamphilis[3], Jessica M. Waite[1], Loren A. Honaas[1*]

1. USDA, ARS, Tree Fruit Research Laboratory, Wenatchee, WA, United States 98801
2. Department of Horticulture, Washington State University, Pullman, WA, United States 99163
3. Department of Biology, The Pennsylvania State University, University Park, PA, United States 16802
4. College of Agriculture, Auburn University, Auburn, AL, United States 36849
5. HudsonAlpha Institute for Biotechnology, Huntsville, AL, United States 35806

Email addresses:

Huiting Zhang: huiting.zhang@wsu.edu ; Eric K. Wafula: ekw10@psu.edu ; Jon Eilers: jon.eilers@usda.gov ; Alex E. Harkess: aharkess@hudsonalpha.org ; Paula E. Ralph: per125@psu.edu ; Prakash Raj Timilsena: prt119@psu.edu; Claude W. dePamphilis: cwd3@psu.edu ; Jessica M. Waite: jessica.waite@usda.gov ; Loren A. Honaas: loren.honaas@usda.gov

* Corresponding author:

Loren A. Honaas

Tree Fruit Research Laboratory, USDA-ARS, 1104 N. Western Ave, Wenatchee, WA 98801

Telephone: 509-664-2280 x 211; Mobile: 509-433-1143; Fax: 509-664-2287

Abstract

The rapid development of sequencing technologies has led to a deeper understanding of horticultural plant genomes. However, experimental evidence connecting genes to important agronomic traits is still lacking in most non-model organisms. For instance, the genetic mechanisms underlying plant architecture are poorly understood in pome fruit trees, creating a major hurdle in developing new cultivars with desirable architecture, such as dwarfing rootstocks in European pear (*Pyrus communis*). Further, the quality and content of genomes vary widely. Therefore, it can be challenging to curate a list of genes with high-confidence gene models across reference genomes. This is often an important first step towards identifying key genetic factors for important traits. Here we present a draft genome of *P. communis* 'd'Anjou' and an improved assembly of the latest *P. communis* 'Bartlett' genome. To study gene families involved in tree architecture in European pear and other rosaceous species, we developed a workflow using a collection of bioinformatic tools towards curation of gene families of interest across genomes. This lays the groundwork for future functional studies in pear tree architecture. Importantly, our workflow can be easily adopted for other plant genomes and gene families of interest.

Introduction

Advancements in plant genome sequencing and assembly have vigorously promoted research in non-model organisms. In horticultural species, new genome sequences are being released every month [1–6]. These genomes have broadened our understanding of targeted cultivars and provided fundamental genomic resources for molecular breeding and more in-depth studies of economically important crop traits such as those involved in plant architecture. Although many

gene families have been identified as important for architectural traits, such as dwarfing, weeping, and columnar growth[7], the study of these genes and their functionality in new species is still hampered by inaccurate information about their gene models or domain structures, and the frequent lack of 1:1 orthology between related genes of different study species. Sequencing and annotating a diversity of related genomes are crucial steps for obtaining this level of information.

Crops, most of which have gone through more than ten thousand years of domestication to meet human requirements, have a wide diversity in forms, sometimes even within the same species[8]. One such example is in the *Brassica* species, where *B. rapa* encompasses morphologically diverse vegetables such as Chinese cabbage, turnips, and mizuna; and cabbage, stem kale, and Brussels sprouts are the same biological species, *B. oleracea*. Therefore, a single reference genome does not represent the complex genome landscape, or pan-genome, for a single crop species. To understand the genetic basis of the diverse *Brassica* morphotypes, many attempts have been made to explore the genomes of *Brassica*[8–12]. In one of those attempts, genomes from 199 *B. rapa* and 119 *B. oleracea* accessions were sequenced and analyzed using a comparative genomic framework[10,12]. Genomic selection signals and candidate genes were identified for traits associated with leaf-heading and tuber-forming morphotypes. Compared to *Brassica*, pome fruits may not appear to have as much diversity in their vegetative appearance, but they do have great diversity in terms of fruit quality, rootstock growth and performance, and post-harvest physiology. However, genome studies and pan-genome scale investigations in pome fruits are still in their infancy. In cultivated apple (*Malus domestica*), genomes of three different cultivars[13–16] have been published, providing resources to study: 1) small (SNPs and small InDels) and large scale (chromosome rearrangements) differences that can help explain cultivar

diversity, and 2) gene content differences that may contribute to cultivar specific traits. However, genomic resources for European pear (*Pyrus communis*) cultivars are limited to just two published genomes[17,18] from a single cultivar, 'Bartlett'. More European pear genomes will afford new perspectives that help us understand shared and unique traits for important cultivars in *Pyrus*, as well as other Rosaceae.

Besides understanding large scale genomic characteristics, new genomes also provide rich resources for reverse genetic studies[19,20]. To obtain the actual sequence of a target gene, reverse genetic approaches in the pre-genome era relied on sequence and domain homology and technologies such as RACE PCR[21], which could be challenging and time consuming. Alternatively, in species with high-quality reference genomes, the annotation is generally considered to contain all the genes and target genes could ideally be identified with a sequence similarity search (*i.e.*, BLAST). However, reports of annotation errors, such as imperfect gene models and missing functional genes are very common[22,23,24]. Another complicating factor is that duplication events (*i.e.*, whole genome duplication, regional tandem duplication) and polyploidy occur in the majority of flowering plants, including most crop species, posing substantial challenges to genome assembly and annotation[25]. Moreover, instances of neofunctionalization and subfunctionalization occur frequently following duplication events[26], which sometimes will result in large and complex gene families[27,28]. Therefore, a one-to-one relationship between a gene in a model organism and its ortholog in other plant species, or even between closely related species and varieties, is rare[29]. Without understanding the orthology and paralogy between members of a given gene family, it is difficult to translate knowledge of a gene in a model organism to another species of interest.

In the present study, we assembled a draft genome for the European pear cultivar 'd'Anjou', improved the current 'Bartlett' assembly (*i.e.*, Bartlett.DH_V2), and developed a workflow that allows highly efficient target gene identification in any plant genome of interest. We used our workflow to curate and improve gene models for architecture-related genes from both the polished Bartlett.DH_v2 and the d'Anjou genomes. Importantly, we recovered many genes that were missing from gene families of interest (50 genes in the cultivar 'Bartlett') and corrected errors in others across the genus *Pyrus*. This work demonstrates that the integration of comparative genomics and phylogenomics can facilitate and enhance gene annotation, and thus gene discovery, in important plant reference genomes.

Results

The draft d'Anjou genome

Genome assembly

We generated approximately 134 million paired-end reads from Illumina HiSeq and a total of 1,054,992 PacBio continuous long reads (CLR) with a read length N50 of 20 Kb, providing an estimated 67-fold and 21-fold coverage respectively of the expected 600 Mb *Pyrus communis* genome[18]. Additionally, approximately 468 million 2 x 150 bp paired reads (~234-fold coverage) with an estimated mean molecule length (linked-reads) of 20 kb were generated using 10x Genomics Chromium Technology (Supplementary Table 1). The final meta-assembly, generated with a combination of the three datasets, contains 5,800 scaffolds with a N50 of 358 Kb (Table 1). The cleaned contigs and scaffolds were ordered and oriented into 17 pseudochromosomes guided by the reference genome, *Pyrus communis* 'Bartlett.DH_v2'[17].

Next, we compared the d'Anjou meta-assembly to two published reference assemblies of Bartlett[17,18] to assess assembly contiguity, completeness, and structural accuracy. The Benchmarking Universal Single-Copy Ortholog (BUSCO)[30] analysis showed that the d'Anjou genome captured 96.6% complete genes in the Embryophyta gene sets, comparable to the reference genomes (Table 1, Supplementary Table 2). Furthermore, synteny comparisons between the draft d'Anjou genome and the reference Bartlett.DH_v2 genome showed high collinearities at both whole-genome and chromosomal levels (Fig. 1a and Supplementary Fig. 1).

Annotation

Combining information such as *de novo* transcriptome assembly, homologous proteins of closely related species, and protein-coding gene annotations from the two Bartlett genomes, we identified a total of 45,981 protein coding genes in d'Anjou (Table 1). Of those putative genes 76.63% were annotated with functional domains from Pfam[31] and the remaining are supported by annotation evidence, primarily d'Anjou RNA-Seq reconstructed transcript[32]. These results indicate that we captured a large majority of the gene space in the d'Anjou genome. This affords a range of analyses including gene and gene family characterization, plus global-scale comparisons with other Rosaceae including the 'Bartlett' cultivar.

Comparison among three European pear genomes

To study the shared and genotype-specific genes among the three European pear genomes, we constructed 25,511 protein clusters, comprising 77.71% of all the genes. While numbers of predicted genes from the Bartlett_v1 and d'Anjou genomes may be overestimated due to the

presence of alternative haplotype segments in the assembly caused by high heterozygosity[17], this should have very little effect on orthogroup circumscription. Further, the process of creating a double haploid reduces genome heterozygosity, but should retain estimates of orthogroup content. Hence, we formulated the following hypotheses: 1) a large majority of gene families are shared by all three genotypes; 2) few genotype-specific gene families are present in each genome; 3) the commercial 'Bartlett' genotype and the double haploid "Bartlett' genotype (roughly version 1.0 and 2.0 of this genome, respectively) should have virtually identical gene family circumscription; and 4) we should detect very few gene families that are unique to either 'Bartlett' genome and shared with 'd'Anjou'. The protein clustering analysis results (Table 1, Fig. 1b) support our hypotheses 1 and 2: 65.60% of the orthogroups contain genes from all three genotypes and only 0.12% of the orthogroups are species-specific. However, among the 8,744 orthogroups containing genes from two genotypes, more than half (55.11%) are shared between d'Anjou and Bartlett_v1, 18.10% are shared by d'Anjou_v1 and Bartlett.DH_v2, and only 26.80% are shared between the two Bartlett genomes, which does not support hypotheses 3 and 4.

To better understand why these hypotheses lacked support, we took a broader look at gene family content by comparing a collection of Rosaceae genomes, including the pear genomes in question. We assigned all the predicted protein coding genes from genomes of interest[13–15,17,18] to orthogroups constructed with a 26-genome scaffold, covering most of the major lineages of land plants (supplementary Fig. 2). Out of the 18,110 orthogroups from this database, *Prunus persica*, a rosaceous species included in the genome scaffold, has representative genes in 10,290 orthogroups. Genes from most apple and pear genomes (Bartlett_v1, d'Anjou_v1, *Malus*

domestica HFTH_v1.0, *M. domestica* GDDH13_v1.1, *M. domestica* Gala_v1.0, *M. sieversii*_v1.0, *M. sylvestris*_v1.0) are present in more than 9,800 orthogroups, however, genes from Bartlett.DH_v2 were only found in 9,688 orthogroups (Table 1 & Supplementary Table 3). These results suggest there are many genes not annotated in the Bartlett.DH_v2 genome.

Genome-Wide identification of selected architecture genes

A selection of architecture genes

With this new comparative genomic information, our next steps were two-fold: first, to leverage information from the three European pear genomes and other available Rosaceae genomes, to identify and improve a set of tree architecture-related gene models of interest, and second, to use these architecture gene families as a test case to investigate potential issues in the Bartlett.DH_v2 genome. Many aspects of tree architecture are important for improving pear growth and maintenance, harvest, ripening, tree size and orchard modernization, disease resistance, and soil microbiome interaction. Traits of interest include dwarfing and dwarfism, root system architecture traits, and branching and branch growth. We selected key gene families known to be involved (Table 2)[33–64], particularly those that have been previously shown to influence architectural traits in fruit trees. The identification of genes within these families, as well as their genomic locations, correct gene models, and domain conservation, is an important early step in testing and understanding their relationships and functions.

Overview of the gene identification workflow

Here, we developed a high throughput workflow (Fig. 2), leveraging a subset of the best Rosaceae plant genomes, and a phylogenomic perspective to efficiently and accurately generate

lists of genes in gene families of interest and phylogenetic relationships of genes from different plant lineages. Our workflow, consisting of three main steps, implemented various functions from PlantTribes[65] (https://github.com/dePamphilis/PlantTribes) and other software [66,67] for targeted gene annotation.

Step 1 - An initial gene list and preliminary phylogenies

In Step 1, representative plant architecture genes obtained from the literature were assigned into orthogroups based on sequence similarity, giving us 22 orthogroups of interest (Supplementary Tables 4-5. Note that OG12636 is a monocot-specific orthogroup, thus not included in the downstream analysis of this section). In parallel, we classified all the genes annotated from 14 Rosaceae genomes (Supplementary Fig. 2) into the same database. Next, Rosaceae genes assigned into the 21 orthogroups were integrated with sequences from the 26 scaffolding species for multiple sequence alignments, which were used to infer phylogeny. At the end of this step, we obtained our initial list of genes in each orthogroup and the phylogenetic relationships of each gene family.

After examining the 21 orthogroups, we identified 64, 105, 94, and 53 genes from *Prunus persica*, Gala_v1, d'Anjou, and Bartlett.DH_v2, respectively. A whole genome duplication (WGD) event occurred in the common ancestor of *Malus* and *Pyrus*[14], but was not shared with *Prunus.* Therefore, we expect to see an approximate 1:2 ratio in gene numbers in most cases, which explains fewer genes in *Prunus* compared to Gala_v1 and d'Anjou. However, the low gene count in Bartlett.DH_v2 was unexpected. For instance, we observed a clade within a PIN orthogroup (OG1145) comprised of short *PIN* genes[38], which seemed to lack genes from the

Bartlett.DH_v2 genome altogether (Fig. 3a). One gene copy is found in *Prunus* and Rosoideae species, and two copies are found in most of the Maleae species, but none were identified in Bartlett.DH_v2. In addition, in the four genomes mentioned above, we found a number of problematic genes (Supplementary Table 6), for example genes that appeared shorter than all other orthologs or contained unexpected indels likely due to assembly or annotation errors.

Step 2 and 3 - Iterative reannotation of problematic gene models

Inaccurate and missing gene models are common in any genome, especially in the early annotation versions[23,24]. In model organisms, such as human, mouse (https://www.gencodegenes.org/), and *Arabidopsis* (https://www.arabidopsis.org/), gene annotations are continuously being improved using experimental evidence, improved data types (*e.g.* full-length RNA molecule sequencing), and both manual and computational curation. Building a better genome assembly is another way to detect additional genes. For instance, the BUSCO completeness score increased from 86.7% in the initial 'Golden Delicious' apple genome[16] to 94.9% in the higher-quality GDDH13 genome[15], indicating that the latter genome captured approximately 120 more conserved single-copy genes. Hence, we hypothesized that the potentially missing and problematic gene models we observed in the two European pears could be improved by: 1) using additional gene annotation approaches; and 2) searching against improved genome assemblies.

To test whether further gene annotation would improve problematic gene models, we moved forward to Step 2 of our workflow, using results from Step 1 as inputs. For each orthogroup containing problematic European pear genes (Supplementary Table 6), we used a subset of high-

quality gene models from Rosids identified in Step 1 as inputs and re-annotated these gene families in the two pear genomes. After using a combination of annotation softwares and manual curation, we found a total of 98 genes from the d'Anjou genome, and reduced the number of problematic or incomplete genes from 34 to 3. In Bartlett.DH_v2, we identified 20 complete genes that were not annotated in the original genome and improved the sequences of 7 previously problematic genes, however, the total number of the selected architecture genes (73 genes among which 15 were problematic or incomplete) was still notably lower than that of d'Anjou (98 with 3 incomplete genes) or Gala (105 with 15 being incomplete, see Supplementary Table 6). In Step 3, which involves iterative steps of phylogenetic analysis and targeted gene re-annotation, we added additional information such as the improved d'Anjou genes and RNA-seq datasets as new resources to annotate Bartlett.DH_v2 genes, but found no improvements in identifying unannotated genes or improving problematic models.

Results gathered after the first iteration of Step 3 supported our hypothesis that extra annotation steps could help improve imperfect gene models and identify missing genes in the two targeted European pear genomes. However, there were still about 30 genes potentially missing in Bartlett.DH_v2, which led us to test whether polishing the genome assembly would further improve problematic or missing gene models.

Step 3 - Adding Bartlett.DH_v2 genome polishing

The quality of genome assembly is affected by many factors, including sequencing depth, contig contiguity, and post-assembly polishing. Attempts to improve a presumably high-quality genome are time consuming, and may prove useless if the genome is already in good condition. To

initially determine whether polishing the genome assembly would be useful, we first investigated the orthogroups with problematic Bartlett.DH_v2 genes to seek for evidence of assembly derived annotation issues. Indeed, in most cases where we failed to annotate a gene from presumably the correct genomic region, we observed unexpected indels while comparing the Bartlett.DH_v2 genome assembly to other pear genomes (Supplementary Fig. 3 and Supplementary Table 7). Unexpected indels in the Bartlett.DH_v2 genome were associated with incorrect gene models as well. For example, Fig. 3b shows a subset of amino acid sequence alignments for a specific member (*Pyrco_BartlettDH_13g21160*) of a PIN orthogroup (OG438) comprised of the long *PIN* genes[38], in which the Bartlett.DH_v2 gene model shared low sequence identity with orthologs from other Maleae species and *Prunus*. To validate the identity of the problematic gene models, we leveraged RNAseq data from various resources[68–73] and mapped them to the Bartlett.DH_v2 gene models. In most cases where a conflict was present between the pear consensus, for a given gene of interest, and the Bartlett.DH_v2 gene model, the reads supported the consensus (Fig. 3c). The frequent occurrence of truncated and missing genes in the Bartlett.DH_v2 genome may be caused by assembly errors (*e.g.*, base call errors, adapter contamination) that create erroneous open reading frames. This observation provided us with the first piece of evidence that the differences in gene family content observed in the Bartlett.DH_v2 genome may not only be caused by misannotations, but also assembly issues.

To further test whether improvement to the genome assembly would allow us to capture the problematic and missing genes, we polished the Bartlett.DH_v2 genome with Illumina reads from the original publication [17]. We identified 98.40% complete BUSCOs in the polished genome assembly, a 1.90% increase compared to the original assembly (Supplementary Table 2).

Using the polished genome, we reiterated Step 3 of our workflow and annotated a total of 103 genes in our gene families of interest, with only two gene models being incomplete (Supplementary Table 6). This new result doubled the number of genes we identified from the original genome annotation and brought the expected gene number into parity with other pome fruit genomes. This supports our hypothesis that genes were missing due to methodological reasons, and in this case, due to assembly errors.

Curation of a challenging gene family: the IGT family

Some gene families are more complex than others. For example, it is more difficult to study the evolution of resistance (R) genes than most BUSCO genes because the former is comprised of fast-evolving multigene families while the latter are universally conserved single-copy gene families. Within the architecture gene families we studied, the IGT family is more challenging than many others because members of this family have relatively low levels of sequence conservation outside of a few conserved domains[74]. Previous reports identified four major clades (LAZY1-like, DRO1-like, TAC1-like, and LAZY5-like) in this gene family[34]. Study of LAZY1 in model species identified 5 conserved regions[74] (Fig 4c). The same domains are also present in other LAZY1-like and DRO1-like proteins and the first 4 domains are found in TAC1-like proteins across land plants[75]. LAZY5-like, the function of which is largely unknown, has only domains I and V. Early research of the *TAC1-like* and *LAZY1-like IGT* genes identified these genes as grass-specific[76,77], as BLAST searches failed to find homologs in other plant lineages.

Using Arabidopsis and rice *IGT* genes as queries, our workflow identified five orthogroups (Supplementary Table 4), containing all the pre-characterized *IGT* genes in angiosperms. The

phylogeny constructed with these five orthogroups largely supported previous classification of the four clades[34], and provided more information regarding the evolutionary history of this gene family (Fig. 4a and Supplementary Fig. 4). The TAC1-like clade, which is sister to the others, is divided into two monophyletic groups; one contains only monocots while the other has representatives from all the other angiosperm lineages. The LAZY1-like and LAZY5-like clades form one large monophyletic group, which is sister to the DRO1-like clade. Within Rosaceae, a near 1:2 ratio was expected between peach and pear due to the WGD in the common ancestor of the Maleaes. Compared to the six known peach *IGT* genes[34], we found 11 orthologs in Bartlett.DH_v2 (including 1 short gene, *Pycro_BartlettDH_LAZY.Chr10*, caused by an unexpected premature stop codon) and 9 in d'Anjou (*Pycro_Danjou_DRO.Chr2* and *Pycro_Danjou_LAZY.Chr10* failed to be annotated due to missing information in the genome). The resulting phylogeny (Fig. 4a) shows that we have now identified most of the expected *IGT* genes in European pears.

Besides low sequence similarity, *IGT* genes also have unique intron-exon arrangements, which are conserved across Arabidopsis and a few other plant species[34,74,78]. These genes all contain 5 exons, but unlike most genes, the first exon only comprises six nucleotides and the last exon contains ~20 nucleotides. Annotation of short exons, especially when transcriptome evidence is limited, can be very challenging and skipping such exons could cause problems in gene discovery[79–81]. For instance, the annotation of *AtAPC11* (*At3g05870*) was inaccurate until Guo and Liu identified a single-nucleotide exon in this gene[80].

To determine whether we captured the correct *IGT* gene models in the targeted genomes, we investigated the protein sequence alignments and gene features. In the original annotation, only three gene models (*Pyrco_BartlettDH_16g10510*, *Pyrco_BartlettDH_07g15250*, *Pyrco_DAnjou_Chr7v0.1_17442.1*) have the correct intron-exon combination and the expected domains. In the iterative re-annotation steps of our workflow, we identified 6 additional accurate gene models leveraging sequence orthology and transcriptome evidence[68–73]. We further investigated all the sequences we identified as *IGT* genes, seeking the presence or absence of the expected domain features. However, even among gene models from the best annotated genomes used to construct the 26Gv2.0 database, only 45.16% (56/124) have the expected domain features (Indicated with an * next to gene names in Fig. 4a) (LAZY5-like was not taken into consideration due to its unique structure). In most cases, although the signature IGT domain (II) is correctly identified in the genes, domains I and V are usually missing or incorrect, likely due to mis-annotation of the first and last short exons. In Rosaceae, besides Bartlett.DH_v2 and d'Anjou, 34.38% (33/96) had the expected domains (Fig. 4a). This finding motivated us to manually investigate the targeted genomes to annotate the IGT genes. Using the correct gene models as reference, plus a careful manual curation, we were able to annotate 19 complete gene models of 20 expected IGT genes from the two targeted pear genomes (Figs. 4b and 4c).

Discussion

A second European pear cultivar genome from 'd'Anjou' provided additional insights into gene families across Rosaceae. By leveraging perspectives from comparative genomics and phylogenomics, we developed a high-throughput workflow using a collection of bioinformatic

343 tools that takes a list of genes of interest from the literature and genomes of interest as input, and
344 produces a curated list of the targeted genes in the query genomes.
345
346 In the case study presented here, candidate genes from 16 plant architecture-related gene families
347 were identified from 14 Rosaceae genomes. The study of gene families consists primarily of two
348 initial parts: first, identification of all the members in these families, and second, investigation of
349 their phylogenetic relationships. Many attempts[82–84] to identify genes of interest from a genome
350 have relied solely on a BLAST search querying a homolog from a model organism, which may
351 be distantly related. However, such a method is insufficient in identifying all members of a large
352 complex gene family or a fast-evolving and highly-divergent family, such as the *IGT* genes.
353 They may also incorrectly include genes in a gene family based only on one or a few highly
354 conserved regions that are insufficient for gene family membership. Compared to a BLAST-only
355 approach, the gene classification process in our workflow used a combination of BLAST and
356 HMMER search of an objectively pre-classified gene family scaffold, which provides a better
357 result by taking into consideration both sensitivity and specificity[65]. This allowed us to
358 efficiently identify even very challenging genes. Moreover, phylogenetic relationships revealed
359 by a small number of taxa, for instance using only one species of interest and one model
360 organism, can be inaccurate. For example, in our phylogenetic analysis with rich taxon sampling,
361 *PIN5-1* and *PIN5-2* from *Pyrus bretschneideri* are sisters to all other *PINs* (Supplementary Fig.
362 5), challenging the phylogenetic relationship inferred with *PINs* only from *P. bretschneideri* and
363 *Arabidopsis thaliana*[61].
364

The iterative quality control steps in the workflow helped identify problems that existed in certain gene models and provided hints about where to make targeted improvements to important *Pyrus* genomic resources. The highly contiguous assembly of Bartlett.DH_v2 provided a valuable reference to anchor the shorter scaffolds from d'Anjou, which is essential for a good annotation. On the other hand, the perspective afforded by the d'Anjou genome led us to examine the Bartlett.DH_v2 genome assembly further. We developed and tested hypotheses regarding unexpected gene annotation patterns in the two targeted European pear genomes among various Maleae species and cultivars. This led to a polished assembly and improved annotations that allowed us to curate a high confidence list of candidate genes and gene models for downstream analyses. By adding targeted iterations of genome assembly and annotation, we now have a better starting point for reverse genetic analyses and understanding functionality of architecture-related genes in pears.

The challenges we encountered as we laid the groundwork for reverse genetics studies to understand pear architecture genes, and the approaches we took to evaluate and tackle these challenges, reinforce the idea that genome assembly and annotation are iterative processes. We found that relating gene accession IDs and inconsistent gene names back to gene sequences in various databases was often difficult and time consuming. Objective, global-scale gene classification, as we used here via PlantTribes[65,85], can help researchers work across genomes and among various genome resources. Further, guidance from consortia such as AgBioData[86] is helping facilitate work such as we have described here that includes the acquisition and analysis of genome-scale data. Our starting point for understanding putative architecture genes in pear was with genes of interest from several plant species - an approach that many researchers will

find familiar. With genes of interest in hand, our workflow provides a comparative genome approach to efficiently identify, investigate, and then improve and/or validate genes of interest across genomes and genome resources.

Materials and Methods

Plant materials and sequencing

The 'd'Anjou' plants were purchased from Van Well's nursery in East Wenatchee, WA, USA and grown in the USDA ARS greenhouse #6 at Wenatchee, WA, USA. Fresh leaves (~1.5g) from one 'd'Anjou' plant were flash frozen and used for DNA extraction. A CTAB isolation protocol[87] was used to generate high-molecular-weight genomic DNA with the following modifications: the extraction was performed large scale in 100 ml of extraction buffer in a 250 ml Nalgene centrifuge bottle; the isopropanol precipitation was performed at room temperature (~ 5 minutes) followed immediately by centrifugation; after a 15-minute incubation in the first pellet wash solution, the pellet was transferred to a 50 ml centrifugation tube via sterile glass hook before performing the second pellet wash; following the second pellet wash, centrifugation and air drying, the pellet was resuspended in 2 ml TE buffer (10 mM Tris, 1 mM EDTA, pH 8.0) and allowed to resuspend at 4 °C overnight. The concentration of the DNA was measured by a Qubit 2.0 fluorometer (Invitrogen) and 50 ug DNA was digested with RNase A (Qiagen, final concentration 10 ug/ml, 37 °C for 30 minutes) and then further cleaned up using the PacBio recommended, user-shared gDNA clean-up protocol (https://www.pacb.com/search/?q=user+shared+protocols) performed at large-scale with the DNA sample brought up to 2 ml with TE and all other volumes scaled up accordingly. The final pellet was resuspended in 100 ul TE. The final DNA concentration was measured by Qubit

fluorometer, and 500 ng was loaded onto a PFG (Bio-Rad CHEF) to check the size range. The DNA ranged in size from 15 Kb to 100 Kb with a mean fragment size around 50 Kb. The purity of the DNA as measured by the NanoDrop spectrophotometer (ThermoFisher) was 260/280 nm: 1.91; 260/230 nm: 2.51. Cleaned-up gDNA was sent to the Penn State Genomics Core facility (University Park, PA, USA) for Pacbio and Illumina library construction and sequencing. A total of 10 ug gDNA was used to construct PacBio SMRTbell libraries and sequenced on a PacBio Sequel system. A small subset of the same gDNA was used to make Illumina TruSeq library and was sequenced on an Illumina HiSeq 2500 platform. In addition, 4 ug of the same gDNA was sent to the DNA technologies and Expression Analysis Core Laboratory at UC Davis (Davis, CA, USA) to construct an Illumina 10X Chromium library, which was sequenced on an Illumina NovaSeq 6000 sequencer.

Genome assembly and post-assembly processing

To create the initial backbone assembly of d'Anjou, Canu assembler v2.1.1[88] was used to correct and trim PacBio continuous long reads (CLR) followed by a hybrid assembly of Illumina short reads and PacBio CLR with MaSuRCA assembler v3.3.2[89]. Next, Supernova v2.1.1, the 10x Genomics *de novo* assembler[90], was used to assemble linked-reads at five different raw read coverage depths of approximately 50x, 59x, 67x, 78x, and 83x based on the kmer estimated genome size, and the resulting phased assembly graph was translated to produce two parallel pseudo-haplotype sequence representations of the genome. The Supernova assembler can only handle raw data between 30- to 85-fold coverage of the estimated genome size. Therefore, the muti-coverage assemblies provide an opportunity to capture most of the genome represented in the ~234-fold coverage sequenced 10x Chromium read data. One of the pseudo-haplotypes at

each of the five coverages was utilized for subsequent meta-assembly construction to improve the backbone assembly using a combination of assembly metrics, including 1) contig and scaffold contiguity (L50), 2) completeness of annotated conserved land plants (embryophyta) single-copy BUSCO genes[30], and 3) an assembly size closer to the expected d'Anjou haploid genome size. The backbone assembly was incrementally improved by bridging gaps and joining contigs with the Quickmerge program[91] using contigs from the five primary Supernova assemblies in decreasing order of assembly quality. The resulting meta-assembly at each merging step was only retained if improvement in contiguity, completeness, and assembly size was observed.

Next, the long-distance information of DNA molecules provided in linked-reads was used to correct assembly errors introduced in the meta-assembly during both the *de novo* and merging steps of the assembly process with Tigmint[92] and ARCS[93] algorithms. Tigmint aligns linked reads to an assembly to identify potential errors and breaks assembled sequences at the boundaries of these errors. The assembly is then re-scaffolded into highly contiguous sequences with ARCS utilizing the long-distance information contained in the linked reads. To further improve the d'Anjou meta-assembly, trimmed paired-reads from both the short insert Illumina and 10x Chromium libraries were utilized to iteratively fill gaps between contigs using GapFiller v1.10[94], and correct base errors and local misassemblies with Pilon v1.23[95]. The genome assembly process is illustrated in Supplementary Fig. 6.

Pseudomolecule construction

Before constructing the d'Anjou nuclear chromosomal-scale pseudomolecules, extraneous DNA sequences present in meta-assembly were identified and excluded (Supplementary Fig. 6). Megablast searches with e-value < 1e-10 was performed against the NCBI nucleotide collection database (nt), and then the best matching Megablast hits (max_target_seqs = 100) against the NCBI taxonomy database were queried to determine their taxonomic attributions. Assembly sequences with all their best-matching sequences not classified as embryophytes (land plants) were considered contaminants and discarded. A second iteration of Megablast searches of all the remaining sequences (embryophytes) was performed against the NCBI RefSeq plant organelles database to identify chloroplast and mitochondrion sequences and assembly sequences with high similarity (> 80% identity; > 50% coverage) to plant organelle sequences were discarded [27,96]. Finally, the remaining meta-assembly nuclear contigs and scaffolds were ordered and oriented into chromosomal-scale pseudomolecules with RaGOO[97] using the European pear, *Pyrus communis* Bartlett.DH_v2 genome[17] reference chromosomes (Supplementary Fig. 6).

Assembly validation

Both the contig and scaffold assembly metrics were evaluated in addition to the completeness of universally conserved single-copy genes using the BUSCO land plants (embryophyta) benchmark gene set (Supplementary Table 8). Whole-genome synteny comparison between Bartlett.DH_v2, the chromosome assembly of the Bartlett cultivar, and d'Anjou meta-assembly were evaluated with D-GENIES[98] using repeat masked (http://www.repeatmasker.org) DNA alignments performed with minimap2[99] for the whole genome and each of the 17 *Pyrus communis* chromosomes as shown in Fig. 1 and Supplementary Fig. 6, respectively.

Gene prediction

To identify the regions of genomic DNA that encode genes, we first estimated the portion of d'Anjou meta-assembly comprised of repetitive elements suitable for repeat masking prior to protein-coding gene annotation following the protocol described by Campbell *et al* (2014)[100]. The meta-assembly was first searched using MITE-Hunter[101] and LTRharvest/ LTRdigest[102,103] to collect consensus miniature inverted-repeat transposable elements (MITEs) and long terminal repeat retrotransposons (LTRs) respectively. LTRs were filtered to remove false positives and elements with nested insertions and used together with the MITEs to mask the genomes. The unmasked regions of the genomes were then annotated with RepeatModeler (http://www.repeatmasker.org/RepeatModeler) to predict additional *de novo* repetitive sequences. All collected repetitive sequences were compared to a BLAST database of plant proteins from SwissProt and RefSeq, and sequences with significant hits were excluded from the repeat masking library.

Extensive extrinsic gene annotation homology evidence from RNA-seq and protein were collected to supplement *ab initio* gene predictions. RNA-Seq evidence included Trinity[104] *de novo* reconstructed transcripts from d'Anjou pear fruit peel and cortex tissues sampled at multiple time points described in our previous study[32]. Protein homology evidence of closely related species were collected from the Genome Database for Rosaceae (GDR), including *Malus domestica*, *Prunus persica*, *Pyrus betulifolia*, *Pyrus communis* 'Bartlett', *Pyrus* x *bretschneideri*, *Rosa chinensis*, and *Rubus occidentalis*[105]. The plant model species, *Arabidopsis thaliana*[106], was included as well.

Protein-coding gene annotations from the *Pyrus communis* reference genomes of Bartlett_v1 and Bartlett.DH_v2 were separately transferred (liftovers) to pseudomolecules of d'Anjou meta-assembly using the FLO (https://github.com/wurmlab/flo) pipeline based on the UCSC Genome Browser Kent-Toolkit[107]. Next, the MAKER annotation pipeline (release 3.01.02)[108] was used to update the transferred annotations with evidence data and gene models predicted by *ab initio* gene finders. Repetitive and low complexity regions of the pseudomolecules were first masked with RepeatMasker in MAKER using the previously described d'Anjou-specific repeat library. MAKER updated transferred annotations with evidence data and predicted additional annotations with Augustus[109,110] and SNAP[111] using the d'Anjou training set where evidence suggests a gene. Only predicted gene models supported by annotation evidence, encode a Pfam domain, or both, were retained.

Computation of pear orthogroups

To compare the gene content of the two *Pyrus communis* cultivars, 'Bartlett' and 'd'Anjou', orthologous and paralogous gene clusters of Bartlett_v1, Bartlett.DH_v2, and d'Anjou were estimated with OrthoFinder version 1.1.5[112] for annotated proteins in all the genomes.

Bartlett.DH_v2 genome polishing

To improve the base quality of the publicly available pear reference genome, the *Pyrus communis* 'Bartlett.DH_v2' assembly was iteratively polished with two rounds of Pilon (v1.24)[95] using the raw Illumina shotgun reads from the Bartlett.DH_v2 genome projects obtained from the NCBI Short Read Archive (SRA accessions: SRR10030340, SRR10030308), and completeness and accuracy assessed with the BUSCO[30] embryophyta_odb10 database.

525

526 **Gene family identification**

527 Coding sequences of candidate genes and their corresponding peptides gleaned from published
528 literature were sorted into pre-computed orthologous gene family clusters of representative 26
529 genomes from land plants using the both BLASTp[113] and HMMER hmmscan[114] sequence search
530 option of the *GeneFamilyClassifier* tool implemented in the PlantTribes gene family analysis
531 pipeline (https://github.com/dePamphilis/PlantTribes). Classification results, including
532 orthogroup taxa gene counts, corresponding superclusters (super orthogroups) at multiple
533 clustering stringencies, and orthogroup-level annotations from multiple public biological
534 functional databases are reported in Supplementary Table 5.

535

536 **Gene family analysis**

537 All the tools used in this process are modules from the command line version of PlantTribes
538 software and are processed on SCINet (https://scinet.usda.gov/) with customized scripts. Protein
539 coding genes from 14 Rosaceae species (*Fragaria vesca* v2.0.a2[115], *Rosa chinensis* old Blush
540 homozygous v2.0[116], *Rubus occidentalis* v3.0[117], *Prunus avium* v1.0.a1[118], *Malus domestica*
541 HFTH v1.0[13], *M. domestica* GDDH13 v1.1[15], *M. domestica* Gala v1.0[14], *M. sieversii* v1.0[14], *M.*
542 *sylvestris* v1.0[14], *Pyrus communis* v1.0[18], *Pyrus communis* Bartlett DH v2.0[17], *Pyrus ussuriensis*
543 x *communis* v1.0[119], *Pyrus bretschneideri* v1.1[120], *Pyrus communis* d'Anjou v0.1) were sorted
544 into orthologous groups with the *GeneFamilyClassifier* as previously described. For species
545 lacking matching coding sequence file and peptide file, transcripts were processed to predict
546 potential protein coding regions using the TransDecoder[121] option of *AssemblyPostProcessor*. A
547 detailed summary of the Rosaceae gene family classification results are in Supplementary Table

3. Sequences classified into the orthogroups of interest (with candidate genes in this study) were integrated with scaffold backbone gene models using the *GeneFamilyIntegrator* tool. Gene names were modified as shown in Supplementary Table 9 for easier recognition of the species. Amino acid multiple sequence alignments and their corresponding DNA codon alignments were generated by *GeneFamilyAligner* with the L-INS-i algorithm implemented in MAFFT[122]. Sites present in less than 10% of the aligned DNA sequences were removed with trimAL[123]. Maximum likelihood (ML) phylogenetic trees were estimated from the trimmed DNA alignments using the RAxML algorithm[124] option in the *GeneFamilyPhylogenyBuilder*. One hundred bootstrap replicates (unless otherwise indicated) were conducted for each tree to estimate the reliability of the branches. The multiple sequence alignments were visualized in the Geneious R9 software[125] with Clustal color scheme. The phylogeny was colored with a custom script and visualized with Dendroscope (version 3.7.5)[126]. Gene sequences, alignments, and phylogenies are available in Supplementary File 1-3.

Domain prediction

To estimate domain structures of proteins in each orthogroup, the predicted amino acid sequences (either obtained from public databases or generated by the PlantTribes *AssemblyPostProcessor* tool) were submitted to interproscan (version 5.44-79.0)[127,128] on SCINet and searched against all the databases.

Targeted gene family annotation

The following approaches were used in parallel to annotate candidate genes from the original Bartlett.DH_v2, polished Bartlett.DH_v2, and the d'Anjou genome assemblies:

571

572 *TGFam-finder*[67]

573 The 'RESOURCE.config' and 'PROGRAM_PATH.config' files were generated according to the
574 author's instruction. The two Bartlett.DH_v2 genome assemblies and the d'Anjou_v1 genome
575 were used as the *target genomes*. Complete protein sequences from apples and pears in the same
576 orthogroup were used as *protein for domain identification*. Complete protein sequences from
577 other Rosaceae species and *Arabidopsis thaliana* in the same orthogroup were used as *resource*
578 *proteins* for each annotation step. For each orthogroup, Pfam annotations from the InterProScan
579 results were used as *TSV for domain identification*. For orthogroups without Pfam descriptions,
580 MobiDBLite information was used as *TSV for domain identification*.

581

582 *Bitacora*[66]

583 Arabidopsis genes from targeted gene families (orthogroups of interest) were used to generate a
584 multiple sequence alignment and HMM profile using MAFFT[122] and hmmbuild. The resulting
585 files were then used as input for Bitacora v1.3, running in both genome mode and full mode to
586 identify genes of interest in the original Bartlett.DH_v2 genome.

587

588 **Manual curation and gene model verification**

589 In cases where both TGFam-Finder and Bitacora failed to predict a full-length gene, the gene
590 model was curated manually.

591

592 *Curation with orthologous gene models*

First, the genomic region containing the target sequence was determined either by the general feature format file (gff) or a BLASTn search using the coding sequence of the target gene or a closely related gene as a query. Next, a genomic fragment containing the target sequence and 3kb upstream and downstream of the targeted region was extracted. Then, the incomplete transcript(s), predicted exons, and complete gene models from a closely related species were mapped to the extracted genomic region. The final gene model was determined by using the full-length coding sequence of a closely related gene as a reference.

Curation with RNA-seq read mapping

The gff3 files obtained from Bitacora were loaded into an Apollo docker container (v2.6.3)[129] for verification of the predicted gene models using expression data. Publicly available RNA-seq data[68–73] for *Pyrus* were used as inputs of an RNA-seq aligner, STAR (v2.7.8a)[130], and alignments were performed with maximum intron size set to 5kb and default settings. Intron-exon structure was compared to the aligned expression data. If there was insufficient RNA-seq coverage from the targeted cultivar, data from other cultivars and *Pyrus* species were used as supporting evidence. Read mapping results are available in Supplementary File 4-5. Curated gene models from the original Bartlett.DH_v2 were transferred to the polished genome for validation.

Gene model cartoons were generated using the visualize gene structure function in TBtools (v1.09854)[131]. Final gene models and their corresponding chromosomal locations are available in Supplementary File 6-7.

Data Availability

Raw read data of d'Anjou genome sequencing has been deposited at NCBI SRA under Bioproject ID PRJNA762155. Genome assembly and gene prediction of the draft 'd'Anjou' genome, and the polished 'Bartlett.DH_v2' genome assembly have been submitted to the Genome Database for Rosacea (GDR). Supplementary information accompanies the manuscript on the BioRxiv.

Acknowledgements

This work was supported by the Washington Tree Fruit Research Commission project PR-17-104 and the Agricultural Research Service in the US Department of Agriculture. The authors would like to acknowledge Heidi Hargarten for maintaining the d'Anjou plant and collecting leaf tissue for sequencing. They also thank Craig Praul at Penn State and Diana Burkart-Waco and Lutz Froenicke at UC Davis for sequencing.

Conflict of interests

The authors declare no conflict of interests.

Author Contributions

HZ, JW, LH conceived and designed the research. PR prepared gDNA for sequencing. HZ, EW, PT, JE, JW, and AH performed the genome assembly and gene family analysis. All authors participated in writing and revising the manuscript.

References

1 Chen, J. *et al.* A chromosome-scale genome sequence of pitaya (*Hylocereus undatus*) provides novel insights into the genome evolution and regulation of betalain biosynthesis. *Hortic Res.* **8**, 164 (2021).

2 Wang, J. *et al*. A high-quality genome assembly of *Morinda officinalis*, a famous native southern herb in the Lingnan region of southern China. *Hortic Res.* **8**, 135 (2021).

3 Huang, Y. *et al*. Genome of a citrus rootstock and global DNA demethylation caused by heterografting. *Hortic Res.* **8**, 69 (2021).

4 Chen, D. *et al*. The chromosome-level reference genome of *Coptis chinensis* provides insights into genomic evolution and berberine biosynthesis. *Hortic Res.* **8**: 121 (2021).

5 Xu, X. *et al*. The chromosome-level *Stevia* genome provides insights into steviol glycoside biosynthesis. *Hortic Res.* **8**: 129 (2021).

6 Wang, P. *et al*. Genetic basis of high aroma and stress tolerance in the oolong tea cultivar genome. *Hortic Res.* **8**: 107 (2021).

7 Hill, J. L. & Hollender, C. A. Branching out: new insights into the genetic regulation of shoot architecture in trees. *Curr Opin Plant Biol*. **47**: 73–80 (2019).

8 Stansell, Z. & Björkman, T. From landrace to modern hybrid broccoli: the genomic and morphological domestication syndrome within a diverse *B. oleracea* collection. *Hortic Res.* **7**: 159 (2020).

9 Stansell, Z. *et al.* Genotyping-by-sequencing of *Brassica oleracea* vegetables reveals unique phylogenetic patterns, population structure and domestication footprints. *Hortic Res.* **5**: 38 (2018).

10 Cheng, F. *et al*. Subgenome parallel selection is associated with morphotype diversification

661 and convergent crop domestication in *Brassica rapa* and *Brassica oleracea*. *Nat Genet.* **48**:
662 1218–1224 (2016).
663 11 Mabry, M. E. *et al*. The evolutionary history of wild, domesticated, and feral *Brassica*
664 *Oleracea* (Brassicaceae). *Mol Biol Evol*. doi:10.1093/molbev/msab183 (2021).
665 12 Cheng, F. *et al*. Genome resequencing and comparative variome analysis in a *Brassica rapa*
666 and *Brassica oleracea* collection. *Sci Data*. **3**: 160119 (2016).
667 13 Zhang, L. *et al*. A high-quality apple genome assembly reveals the association of a
668 retrotransposon and red fruit colour. *Nat Commun.* **10**: 1494 (2019).
669 14 Sun, X. *et al*. Phased diploid genome assemblies and pan-genomes provide insights into the
670 genetic history of apple domestication. *Nat Genet.* **52**: 1423–1432 (2020).
671 15 Daccord, N. *et al*. High-quality *de novo* assembly of the apple genome and methylome
672 dynamics of early fruit development. *Nat Genet.* **49**: 1099–1106 (2017).
673 16 Velasco, R. *et al*. The genome of the domesticated apple (*Malus* × *domestica* Borkh.). *Nat*
674 *Genet.* **42**: 833–839 (2010).
675 17 Linsmith, G. *et al*. Pseudo-chromosome-length genome assembly of a double haploid
676 “Bartlett” pear (*Pyrus communis* L.). *Gigascience.* **8**. doi:10.1093/gigascience/giz138 (2019).
677 18 Chagné, D. *et al*. The draft genome sequence of European pear (*Pyrus communis* L.
678 ‘Bartlett’). *Plos One*. **9**: e92644 (2014).
679 19 Wu, J. *et al*. A naturally occurring InDel variation in *BraA.FLC.b* (*BrFLC2*) associated with
680 flowering time variation in *Brassica rapa*. *Bmc Plant Biol.* **12**: 151 (2012).
681 20 Tollenaere, R. *et al*. Identification and characterization of candidate *Rlm4* blackleg resistance
682 genes in *Brassica napus* using next□generation sequencing. *Plant Biotechnol J*. **10**: 709–715
683 (2012).

684 21 Takos, A. M. *et al*. Light-Induced Expression of a *MYB* Gene Regulates Anthocyanin
685 Biosynthesis in Red Apples. *Plant Physiology* **142**: 1216–1232 (2006).
686 22 Pertea, M. *et al*. CHESS: a new human gene catalog curated from thousands of large-scale
687 RNA sequencing experiments reveals extensive transcriptional noise. *Genome Biol* **19**: 208
688 (2018).
689 23 Pilkington, S. M. *et al*. A manually annotated *Actinidia chinensis* var. *chinensis* (kiwifruit)
690 genome highlights the challenges associated with draft genomes and gene prediction in plants.
691 *Bmc Genomics* **19**: 257 (2018).
692 24 Marx, H. *et al*. A proteomic atlas of the legume *Medicago truncatula* and its nitrogen-fixing
693 endosymbiont *Sinorhizobium meliloti*. *Nat Biotechnol*. **34**: 1198–1205 (2016).
694 25 Kyriakidou, M., Tai, H. H., Anglin, N. L., Ellis, D., & Strömvik, M. V. Current strategies of
695 polyploid plant genome sequence assembly. *Front Plant Sci*. **9**: 1660 (2018).
696 26 Hughes, T. E., Langdale, J. A., & Kelly, S. The impact of widespread regulatory
697 neofunctionalization on homeolog gene evolution following whole-genome duplication in maize.
698 *Genome Res.* **24**: 1348–1355 (2014).
699 27 Yoshida, S. *et al*. Genome sequence of *Striga asiatica* provides insight into the evolution of
700 plant parasitism. *Curr Biol*. **29**: 3041-3052.e4 (2019).
701 28 Yang, Z. *et al*. Comparative transcriptome analyses reveal core parasitism genes and suggest
702 gene duplication and repurposing as sources of structural novelty. *Mol Biol Evol*. **32**: 767–790
703 (2015).
704 29 Xiao, D. *et al*. The *Brassica rapa FLC* homologue *FLC2* is a key regulator of flowering time,
705 identified through transcriptional co-expression networks. *J Exp Bot*. **64**: 4503–4516 (2013).
706 30 Manni, M., Berkeley, M. R., Seppey, M., Simão, F. A., & Zdobnov, E. M. BUSCO update:

novel and streamlined workflows along with broader and deeper phylogenetic coverage for scoring of eukaryotic, prokaryotic, and viral genomes. *Mol Biol Evol*. msab199- (2021).

31 Mistry, J. *et al*. Pfam: The protein families database in 2021. *Nucleic Acids Res*. **49**: gkaa913- (2020).

32 Honaas, L. *et al*. Transcriptomics of differential ripening in 'd'Anjou' pear (*Pyrus communis* L.). *Front Plant Sci*. **12**: 609684 (2021).

33 Kwon, M. & Choe, S. Brassinosteroid biosynthesis and dwarf mutants. *J Plant Biol*. **48**: 1 (2004).

34 Waite, J. M. & Dardick, C. The roles of the *IGT* gene family in plant architecture: past, present, and future. *Curr Opin Plant Biol*. **59**: 101983 (2021).

35 Bulley, S. M. *et al.* Modification of gibberellin biosynthesis in the grafted apple scion allows control of tree height independent of the rootstock. *Plant Biotechnol J*. **3**: 215–223 (2005).

36 Griffiths, J. *et al*. Genetic Characterization and Functional Analysis of the *GID1* Gibberellin Receptors in Arabidopsis. *Plant Cell Online* **18**: 3399–3414 (2006).

37 Dugardeyn, J. & Straeten, D. V. D. Ethylene: Fine-tuning plant growth and development by stimulation and inhibition of elongation. *Plant Sci*. **175**: 59–70 (2008).

38 Křeček, P. *et al*. The PIN-FORMED (PIN) protein family of auxin transporters. *Genome Biol*. **10**: 249 (2009).

39 Martín□Rejano, E. M. *et al*. Auxin and ethylene are involved in the responses of root system architecture to low boron supply in Arabidopsis seedlings. *Physiol Plantarum.* **142**: 170–178 (2011).

40 Li, H. L. *et al*. Possible roles of auxin and zeatin for initiating the dwarfing effect of M9 used as apple rootstock or interstock. *Acta Physiol Plant*. **34**: 235–244 (2012).

730 41 Chang, L., Ramireddy, E., & Schmülling, T. Lateral root formation and growth of
731 Arabidopsis is redundantly regulated by cytokinin metabolism and signalling genes. *J Exp Bot*.
732 **64**: 5021–5032 (2013).
733 42 Dardick, C. *et al*. *PpeTAC1* promotes the horizontal growth of branches in peach trees and is
734 a member of a functionally conserved gene family found in diverse plants species. *Plant J*. **75**:
735 618–630 (2013).
736 43 Tworkoski, T., Webb, K., & Callahan, A. Auxin levels and *MAX1–4* and *TAC1* gene
737 expression in different growth habits of peach. *Plant Growth Regul.* **77**: 279–288 (2015).
738 44 Hollender, C. A., Hadiarto, T., Srinivasan, C., Scorza, R., & Dardick, C. A brachytic
739 dwarfism trait (*dw*) in peach trees is caused by a nonsense mutation within the gibberellic acid
740 receptor *PpeGID1c*. *New Phytol.* **210**: 227–239 (2016).
741 45 Ma, Y. *et al*. Involvement of auxin and brassinosteroid in dwarfism of autotetraploid apple
742 (*Malus* × *domestica*). *Sci Rep-uk.* **6**: 26719 (2016).
743 46 Li, G. *et al*. Transcriptome analysis reveals the effects of sugar metabolism and auxin and
744 cytokinin signaling pathways on root growth and development of grafted apple. *Bmc Genomics.*
745 **17**: 150 (2016).
746 47 Foster, T. M., McAtee, P. A., Waite, C. N., Boldingh, H. L., & McGhie, T. K. Apple
747 dwarfing rootstocks exhibit an imbalance in carbohydrate allocation and reduced cell growth and
748 metabolism. *Hortic Res.* **4**: 17009 (2017).
749 48 Harrison C. J. Auxin transport in the evolution of branching forms. *New Phytol.* **215**: 545–
750 551 (2017).
751 49 Guseman, J. M., Webb, K., Srinivasan, C., & Dardick, C. *DRO1* influences root system
752 architecture in Arabidopsis and *Prunus* species. *Plant J*. **89**: 1093–1105 (2017).

753 50 An, H. *et al*. Dwarfing effect of apple rootstocks is intimately associated with low number of
754 fine roots. *Hortscience*. **52**: 503–512 (2017).
755 51 An, J. *et al*. Molecular cloning and functional characterization of *MdPIN1* in apple. *J Integr*
756 *Agr*. **16**: 1103–1111 (2017).
757 52 Zheng, L. *et al*. Genome-wide identification and expression analysis of brassinosteroid
758 biosynthesis and metabolism genes regulating apple tree shoot and lateral root growth. *J Plant*
759 *Physiol*. **231**: 68–85 (2018).
760 53 Gan, Z. *et al*. *MdPIN1b* encodes a putative auxin efflux carrier and has different expression
761 patterns in BC and M9 apple rootstocks. *Plant Mol Biol.* **96**: 353–365 (2018).
762 54 Zheng, X. *et al*. *MdWRKY9* overexpression confers intensive dwarfing in the M26 rootstock
763 of apple by directly inhibiting brassinosteroid synthetase *MdDWF4* expression. *New Phytol*. **217**:
764 1086–1098 (2018).
765 55 Wang, L. *et al*. The isolation of the *IGT* family genes in *Malus* × *domestica* and their
766 expressions in four idiotype apple cultivars. *Tree Genet Genomes.* **14**: 46 (2018).
767 56 Cheng, J. *et al*. A single nucleotide mutation in *GID1c* disrupts its interaction with *DELLA1*
768 and causes a GA□insensitive dwarf phenotype in peach. *Plant Biotechnol J.* **17**: 1723–1735
769 (2019).
770 57 Li, C. *et al*. Comprehensive expression analysis of Arabidopsis *GA2-oxidase* genes and their
771 functional insights. *Plant Sci.* **285**: 1–13 (2019).
772 58 Zheng, X., Zhang, H., Xiao, Y., Wang, C., & Tian, Y. Deletion in the promoter of *PcPIN-L*
773 affects the polar auxin transport in dwarf pear (*Pyrus communis* L.). *Sci Rep-uk.* **9**: 18645 (2019).
774 59 Swarup, R. & Bhosale, R. Developmental roles of *AUX1/LAX* auxin influx carriers in plants.
775 *Front Plant Sci*. **10**: 1306 (2019).

776 60 Tan, M. *et al*. Role of cytokinin, strigolactone, and auxin export on outgrowth of axillary
777 buds in apple. *Front Plant Sci.* **10**: 616 (2019).
778 61 Qi, L. *et al*. Characterization of the auxin efflux transporter PIN proteins in pear. *Plants.* **9**:
779 349 (2020).
780 62 Sun, X. *et al*. Genes involved in strigolactone biosyntheses and their expression analyses in
781 columnar apple and standard apple. *Biol Plantarum.* **64**: 68–76 (2020).
782 63 Cheng, J. *et al*. Functional analysis of the *Gibberellin 2-oxidase* gene family in peach. *Front*
783 *Plant Sci.* **12**: 619158 (2021).
784 64 Pandey, B. K. *et al*. Plant roots sense soil compaction through restricted ethylene diffusion.
785 *Science* **371**: 276–280 (2021).
786 65 Wafula E. K. Computational methods for comparative genomics of non-model species: A
787 case study in the parasitic plant family Orobanchaceae. (The Pennsylvania State University, State
788 College, PA, USA, 2019).
789 66 Vizueta, J., Sánchez□Gracia, A., & Rozas, J. bitacora: A comprehensive tool for the
790 identification and annotation of gene families in genome assemblies. *Mol Ecol Resour*. **20**:
791 1445–1452 (2020).
792 67 Kim, S. *et al*. TGFam□Finder: a novel solution for target□gene family annotation in plants.
793 *New Phytol*. **227**: 1568–1581 (2020).
794 68 Nham, N. T. *et al*. A transcriptome approach towards understanding the development of
795 ripening capacity in ‘Bartlett’ pears (*Pyrus communis* L.). *Bmc Genomics.* **16**: 762 (2015).
796 69 Hewitt, S. L., Hendrickson, C. A., & Dhingra, A. Evidence for the involvement of
797 vernalization-related genes in the regulation of cold-induced ripening in ‘d’Anjou’ and ‘Bartlett’
798 pear fruit. *Sci Rep-uk.* **10**: 8478 (2020).

799 70 Gabay, G. *et al*. Transcriptome analysis and metabolic profiling reveal the key role of α-
800 linolenic acid in dormancy regulation of European pear. *J Exp Bot.* **70**: ery405 (2018).
801 71 Zhang, Z. *et al*. Transcriptomic and metabolomic analysis provides insights into anthocyanin
802 and procyanidin accumulation in pear. *Bmc Plant Biol.* **20**: 129 (2020).
803 72 Nham, N. T., Macnish, A. J., Zakharov, F., & Mitcham, E. J. 'Bartlett' pear fruit (*Pyrus*
804 *communis* L.) ripening regulation by low temperatures involves genes associated with jasmonic
805 acid, cold response, and transcription factors. *Plant Sci.* **260**: 8–18 (2017).
806 73 Zhang, H. *et al.* RNA-Seq analysis of the tissue-specific expressed genes of *Pyrus*
807 *betulaefolia* in root, stem and leaf. *Acta Horticulturae Sinica*. **45**: 1881–1894 (2018).
808 74 Yoshihara, T., Spalding, E. P., & Iino, M. *AtLAZY1* is a signaling component required for
809 gravitropism of the *Arabidopsis thaliana* inflorescence. *Plant J.* **74**: 267–279 (2013).
810 75 Yoshihara, T., & Spalding, E. P. *LAZY* genes mediate the effects of gravity on auxin
811 gradients and plant architecture. *Plant Physiol*. **175**: 959–969 (2017).
812 76 Li, P. *et al*. *LAZY1* controls rice shoot gravitropism through regulating polar auxin transport.
813 *Cell Res.* **17**: 402–410 (2007).
814 77 Yu, B. *et al*. *TAC1*, a major quantitative trait locus controlling tiller angle in rice. *Plant J.* **52**:
815 891–898 (2007).
816 78 Uga, Y. *et al*. Control of root system architecture by *DEEPER ROOTING 1* increases rice
817 yield under drought conditions. *Nat Genet.* **45**: 1097–1102 (2013).
818 79 Mount, S. M. Genomic sequence, splicing, and gene annotation. *Am J Hum Genetics.* **67**:
819 788–792 (2000).
820 80 Guo, L., & Liu, C-M. A single-nucleotide exon found in Arabidopsis. *Sci Rep-uk.* **5**: 18087
821 (2015).

822 81 Sharma, S., Sharma, S. N., & Saxena, R. Identification of short exons disunited by a short
823 intron in eukaryotic DNA regions. *Ieee Acm Transactions Comput Biology Bioinform.* **17**: 1660–
824 1670 (2018).
825 82 Zheng, X., Xiao, Y., Tian, Y., Yang, S., & Wang, C. *PcDWF1*, a pear brassinosteroid
826 biosynthetic gene homologous to *AtDWARF1*, affected the vegetative and reproductive growth of
827 plants. *Bmc Plant Biol.* **20**: 109 (2020).
828 83 Cancino-García, V. J., Ramírez-Prado, J. H., & De-la-Peña, C. Auxin perception in *Agave* is
829 dependent on the species' Auxin Response Factors. *Sci Rep-uk.* **10**: 3860 (2020).
830 84 Feng, Y. *et al*. Genome-wide identification and characterization of ABC transporters in nine
831 Rosaceae species identifying *MdABCG28* as a possible cytokinin transporter linked to dwarfing.
832 *Int J Mol Sci.* **20**: 5783 (2019).
833 85 Wall, P. K. *et al*. PlantTribes: a gene and gene family resource for comparative genomics in
834 plants. *Nucleic Acids Res.* **36**: D970–D976 (2008).
835 86 Harper, L. *et al*. AgBioData consortium recommendations for sustainable genomics and
836 genetics databases for agriculture. *Database*. **2018**: 1–32 (2018).
837 87 Michiels, A., Ende, W. V. den., Tucker, M., Riet, L. V., & Laere, A. V. Extraction of high-
838 quality genomic DNA from latex-containing plants. *Anal Biochem.* **315**: 85–89 (2003).
839 88 Koren, S. *et al*. Canu: scalable and accurate long-read assembly via adaptive k-mer weighting
840 and repeat separation. *Genome Res.* **27**: 722–736 (2017).
841 89 Zimin, A. V. *et al.* The MaSuRCA genome assembler. *Bioinformatics.* **29**: 2669–2677
842 (2013).
843 90 Weisenfeld, N. I., Kumar, V., Shah, P., Church, D. M., & Jaffe, D. B. Direct determination of
844 diploid genome sequences. *Genome Res.* **27**: 757–767 (2017).

845 91 Chakraborty, M., Baldwin-Brown, J. G., Long, A. D., & Emerson, J. J. Contiguous and
846 accurate *de novo* assembly of metazoan genomes with modest long read coverage. *Nucleic Acids*
847 *Res.* **44**: e147–e147 (2016).
848 92 Jackman, S. D. *et al*. Tigmint: correcting assembly errors using linked reads from large
849 molecules. *Bmc Bioinformatics.* **19**: 393 (2018).
850 93 Yeo, S., Coombe, L., Warren, R. L., Chu, J., & Birol, I. ARCS: scaffolding genome drafts
851 with linked reads. *Bioinformatics.* **34**: 725–731 (2017).
852 94 Boetzer, M. & Pirovano, W. Toward almost closed genomes with GapFiller. *Genome Biol.*
853 **13**: R56 (2012).
854 95 Walker, B. J. *et al*. Pilon: An integrated tool for comprehensive microbial variant detection
855 and genome assembly improvement. *Plos One*. **9**: e112963 (2014).
856 96 Hämälä, T. *et al*. Genomic structural variants constrain and facilitate adaptation in natural
857 populations of *Theobroma cacao*, the chocolate tree. *PNAS.* doi:10.1073/pnas.2102914118
858 (2021).
859 97 Alonge, M. *et al*. RaGOO: fast and accurate reference-guided scaffolding of draft genomes.
860 *Genome Biol*. **20**: 224 (2019).
861 98 Cabanettes, F. & Klopp, C. D-GENIES: dot plot large genomes in an interactive, efficient
862 and simple way. *Peerj.* **6**: e4958 (2018).
863 99 Li H. Minimap and miniasm: fast mapping and *de novo* assembly for noisy long sequences.
864 *Bioinformatics.* **32**: 2103–2110 (2016).
865 100 Campbell, M. S., Holt, C., Moore, B., & Yandell, M. Genome annotation and curation using
866 MAKER and MAKER□P. *Curr Protoc Bioinform.* **48**: 4.11.1-4.11.39 (2014).
867 101 Han, Y. & Wessler, S. R. MITE-Hunter: a program for discovering miniature inverted-

repeat transposable elements from genomic sequences. *Nucleic Acids Res.* **38**: e199–e199 (2010).

102 Ellinghaus, D., Kurtz, S., & Willhoeft, U. LTRharvest, an efficient and flexible software for *de novo* detection of LTR retrotransposons. *Bmc Bioinformatics.* **9**: 18 (2008).

103 Steinbiss, S., Willhoeft, U., Gremme, G., & Kurtz, S. Fine-grained annotation and classification of *de novo* predicted LTR retrotransposons. *Nucleic Acids Res.* **37**: 7002–7013 (2009).

104 Grabherr, M. G. *et al*. Full-length transcriptome assembly from RNA-Seq data without a reference genome. *Nat Biotechnol.* **29**: 644–652 (2011).

105 Jung, S. *et al*. 15 years of GDR: New data and functionality in the Genome Database for Rosaceae. *Nucleic Acids Res*. **47**: D1137–D1145 (2018).

106 Cheng, C. *et al*. Araport11: a complete reannotation of the *Arabidopsis thaliana* reference genome. *Plant J*. **89**: 789–804 (2017).

107 Kuhn, R. M., Haussler, D., & Kent, W. J. The UCSC genome browser and associated tools. *Brief Bioinform.* **14**: 144–161 (2013).

108 Cantarel, B. L. *et al*. MAKER: An easy-to-use annotation pipeline designed for emerging model organism genomes. *Genome Res.* **18**: 188–196 (2008).

109 Stanke, M., Steinkamp, R., Waack, S., & Morgenstern, B. AUGUSTUS: a web server for gene finding in eukaryotes. *Nucleic Acids Res*. **32**: W309–W312 (2004).

110 Hoff, K. J. & Stanke, M. Predicting genes in single genomes with AUGUSTUS. *Curr Protoc Bioinform.* **65**: e57 (2019).

111 Korf, I. Gene finding in novel genomes. *Bmc Bioinformatics.* **5**: 59 (2004).

112 Emms, D. M. & Kelly, S. OrthoFinder: phylogenetic orthology inference for comparative genomics. *Genome Biol.* **20**: 238 (2019).

113 Camacho, C. *et al*. BLAST+: architecture and applications. *Bmc Bioinformatics.* **10**: 421 (2009).

114 Eddy, S. R. Accelerated Profile HMM Searches. *Plos Comput Biol*. **7**: e1002195 (2011).

115 Li, Y. *et al*. Genome re-annotation of the wild strawberry *Fragaria vesca* using extensive Illumina- and SMRT-based RNA-seq datasets. *Dna Res.* **25**: dsx038 (2017).

116 Raymond, O. *et al*. The *Rosa* genome provides new insights into the domestication of modern roses. *Nat Genet.* **50**: 772–777 (2018).

117 VanBuren, R. *et al*. A near complete, chromosome-scale assembly of the black raspberry (*Rubus occidentalis*) genome. *Gigascience*. **7**: giy094- (2018).

118 Shirasawa, K. *et al*. The genome sequence of sweet cherry (*Prunus avium*) for use in genomics-assisted breeding. *Dna Res.* **24**: dsx020- (2017).

119 Ou, C. *et al*. A *de novo* genome assembly of the dwarfing pear rootstock Zhongai 1. *Sci Data* **6**: 281 (2019).

120 Xue, H. *et al*. Chromosome level high-density integrated genetic maps improve the *Pyrus bretschneideri* 'DangshanSuli' v1.0 genome. *Bmc Genomics.* **19**: 833 (2018).

121 Haas, B. J. *et al*. *De novo* transcript sequence reconstruction from RNA-seq using the Trinity platform for reference generation and analysis. *Nat Protoc.* **8**: 1494-1512 (2013).

122 Katoh, K., Misawa, K., Kuma, K., & Miyata, T. MAFFT: a novel method for rapid multiple sequence alignment based on fast Fourier transform. *Nucleic Acids Res.* **30**: 3059–3066 (2002).

123 Capella-Gutiérrez, S., Silla-Martínez, J. M., & Gabaldón, T. trimAl: a tool for automated alignment trimming in large-scale phylogenetic analyses. *Bioinformatics.* **25**: 1972–1973 (2009).

124 Stamatakis, A. RAxML version 8: a tool for phylogenetic analysis and post-analysis of large phylogenies. *Bioinformatics.* **30**: 1312–1313 (2014).

914 125 Kearse, M. *et al*. Geneious Basic: An integrated and extendable desktop software platform
915 for the organization and analysis of sequence data. *Bioinformatics.* **28**: 1647–1649 (2012).
916 126 Huson, D. H., & Scornavacca, C. Dendroscope 3: An interactive tool for rooted
917 phylogenetic trees and networks. *Systematic Biol*. **61**: 1061–1067 (2012).
918 127 Mulder, N. & Apweiler, R. Comparative Genomics. *Methods Mol Biology*. **396**: 59–70
919 (2007).
920 128 Quevillon, E. *et al*. InterProScan: protein domains identifier. *Nucleic Acids Res.* **33**: W116–
921 W120 (2005).
922 129 Dunn, N. A. *et al*. Apollo: Democratizing genome annotation. *Plos Comput Biol.* **15**:
923 e1006790 (2019).
924 130 Dobin, A. *et al*. STAR: ultrafast universal RNA-seq aligner. *Bioinformatics*. **29**: 15–21
925 (2013).
926 131 Chen, C. *et al*. TBtools: An integrative toolkit developed for interactive analyses of big
927 biological data. *Mol Plant*. **13**: 1194–1202 (2020).

928 **Figure legends**

929 **Fig 1. Characterization of the d'Anjou_v1 genome and protein orthology among European**
930 **pears. a.** Dot plot of genome alignment of Bartlett.DH_v2 (x axis) and d'Anjou_v1 (y axis). **b.**
931 Overlap and distinctiveness of gene annotations among three *Pyrus communis* genotypes,
932 Bartlett_v1, Bartlett.DH_v2, and d'Anjou.

933

934 **Fig 2. A workflow for candidate gene identification, curation, and gene family construction.**
935 Grey dotted boxes outlined the three steps of this workflow. Boxes with green outlines are input
936 information. Boxes with blue outlines are intermediate outputs and boxes with purple outlines
937 are final outputs. Contents in boxes with orange outlines are softwares used for generating the
938 outputs.

939

940 **Fig 3. Phylogeny, amino acid sequence comparison, and RNAseq read mapping of *PIN***
941 **genes. a.** One clade of short *PINs* from OG1145 phylogeny. *Malus* genes are indicated with a
942 blue background, *Pyrus* with a green background, and *Prunus* with a pink background. **b.** Amino
943 acid sequence alignment of orthologous genes from 10 Amygdaloideae species in the long *PIN*
944 gene family (OG438). Sites identical to the consensus are shown in grey and sites different from
945 the consensus are shown with a color following the Clustal color scheme in Geneious. Green
946 color in the identity row indicates 100% identical across all sequences and greeny-brown color
947 indicates identity from > 30% to < 100% identity. Gaps in the alignment are shown with a
948 straight line. **c.** RNAseq reads (forward: red; reverse: blue) mapped to a fragment of
949 chromosome 13 in the Bartlett.DH_v2 genome, where a long *PIN* gene,
950 *Pyrco_BartlettDH_13g21160*, was annotated. Gene model in the yellow box is a putative gene

model predicted with RNAseq reads (ref. 73) mapped to this region. The two gene models above the read mapping are retrieved from the original annotations of Bartlett_v1 (*Pyrco_Bartlett_017869.1*) and Bartlett.DH_v2 (*Pyrco_BartlettDH_13g21160*).

Fig 4. Phylogeny, intron-exon structure, and amino acid comparison of IGT genes. a. Cladogram of the IGT gene family (including LAZY1-like, LAZY5-like, TAC1-like, and DRO-like). Genes are colored as shown in Supplementary Fig. 2. 1000 bootstrap replicates were conducted to estimate reliability and the numbers on the node indicate bootstrap support. **b.** Cartoon illustrating intron-exon structures of IGT genes from *Arabidopsis thaliana* (Araport11), Bartlett.DH_v2, and d'Anjou. **c.** Amino acid alignment of IGT genes from *Arabidopsis thaliana*, Bartlett.DH_v2, and d'Anjou. Sites consisting of a similar amino acid type as the consensus were highlighted with a background color following the Clustal color scheme in Geneious. Red color in the identity row indicates identity < 30%. Five conserved regions were highlighted with a grey symbol below the consensus sequence.

966 # Tables

967 **Table 1. Comparison of genome assembly and annotation, and orthogroups among *Pyrus communis***
968 **genotypes.**
969

Characteristics	Bartlett_v1	Bartlett.DH_v2	d'Anjou_v1
Assembly			
Assembly size (Mb)	600	507.7	600
Number of scaffolds	142,083	592	5800
Scaffold N50	88 Kb	8.1 Mb	358.88 Kb
Pseudochromosomes	17	17	17
Annotation			
Predicted gene number	43,419	37,445	45,981
BUSCO	96.5%	96.5%	96.6%
Mean CDS length	1209	1120	1343
Gene family classification			
Percentage of genes classified into pear orthogroups	76.2	76.2	80.4
Percentage of pear orthogroups containing genes	93.7	81	90.7
Number of 26Gv2 orthogroups containing genes	9878	9668	9837

970
971 **Table 2. Architecture gene family table**

Family/ Gene	Species	Gene ID	Cultivar/Ecotype	Method	Associated Architecture Phenotype	Refs
PIN						
PIN1	Apple (*Malus domestica*)	*MdPIN1*: *MDP0000138035* (*M. domestica* genome v1.0)	Royal Gala	Overexpression of *Malus PIN1* gene in Arabidopsis	Inhibition of primary root elongation, increased lateral root number, enhanced phototropic and geotropism responses.	[51]
		MdPIN1a: *MF506847* *MdPIN1b*: *MF506848* (Genbank)	Rootstocks: Baleng Crab, M9; Interstems: M9; Scion: Red Fuji	Comparative gene expression between cultivars; subcellular localization; overexpression in tobacco; IAA	Lower *MdPIN1b* expression in bark of M9 dwarfing rootstock and interstem; longer lateral roots, more adventitious roots, shorter and fewer root hairs in *MdPIN1b*-overexpressing tobacco	[53]

				quantification	lines.	
	Pear (*Pyrus communis*, *P. bretschneideri*)	*PcPIN-L*: *PCP021016* (*P. communis* genome v1.0)	Aihuali x Chili' (*P. bretschneideri* Rehd.), Aihuali, Chili	Comparative gene expression between cultivars, across tissue types; subcellular localization; promoter activity; overexpression in tobacco, IAA quantification	Lower *PcPIN-L* expression in leaves, stems, roots, and seeds of pears exhibiting dwarfism; higher IAA content in shoot tips and lower IAA content in stems of pears exhibiting dwarfism; taller plants with longer cells in the stem, longer and more lateral roots in *PcPIN-L* overexpressing tobacco lines	[58]
PIN1, PIN3	Apple (*Malus robusta*, *M. spectabilis*)	*MrPIN1*: *MDP0000138035* *MrPIN3*: *MDP0000497581* (*M. domestica* genome v1.0)	Rootstock: *M. robusta* Scion: *M. specitabilis* Bly114 (Standard) and more-branching mutant (*MB*)	Gene expression (transcriptome and qPCR) and phenotypes of grafted plants, sugar and hormone quantification across tissues	The more-branching (*MB*) mutant repressed rootstock growth, and glycolysis and tricarboxylic acid activities. Rootstocks grafted with MB showed reduced *MrPIN1* expression, and increased *MrPIN3* expression.	[46]
PIN family	Pear (*Pyrus bretschneideri*, *P. betulifolia*, *P. communis*)	*PbPIN1-1*: *LOC103946937* *PbPIN1-2*: *LOC103950573* *PbPIN1-3*: *LOC103933990* *PbPIN1-4*: *LOC103960490* *PbPIN2-1*: *LOC103941631* *PbPIN2-2*: *LOC103950477* *PbPIN3-1*: *LOC103947028* *PbPIN3-2*: *LOC103948593* *PbPIN3-3*: *LOC103948670* *PbPIN4*: *LOC103931858* *PbPIN5-1*:	Rootstock: Douli Interstems: OHF51, QN101 Scion: Xueqing	Comparative gene expression between cultivars	Compared *PbPIN* gene expression among different tissues of dwarfing OHF51 and vigorous QN101 rootstock cultivars, finding differential expression across tissues. Many *PbPINs* had higher shoot tip expression in the dwarfing rootstocks.	[61]

		LOC103930394 *PbPIN5-2*: *LOC103938552* *PbPIN6*: *LOC103951142* *PbPIN8*: *LOC103934837* (Genbank)				
	Arabidopsis	*AtPIN1: At1g73590* *AtPIN2: At5g57090* *AtPIN3: At1g70940* *AtPIN4: At2g01420* *AtPIN5: At5g16530* *AtPIN6: At2g77110* *AtPIN7: At1g23080* *AtPIN8: At5g15100* (TAIR10)		Review of PIN protein evolution, protein structure, genomic structure, expression patterns, subcellular mechanisms, mutant phenotypes	Mutations in one or more *PIN* genes can lead to pin-like inflorescences, floral defects, gravitropism defects in the shoot or root, fused leaves or cotyledons, and loss of apical-basal patterning.	[38]
	Across kingdom		All plants	Review of the role of auxin transport in branching forms across the plant kingdom	PIN proteins, via polar auxin transport, regulate branch initiation. branch outgrowth, and branch angle in flowering plants.	[48]
AUX/LAX						
AUX1, LAX2	Apple (*Malus domestica*)	*MdLAX2*: *MDP0000020317, MDP0000155074* *MdAUX1*: *MDP0000155113* (*M. domestica* genome v1.0)	Rootstock: M9, M27, M793 Scion: Royal Gala	Gene expression (transcriptome and qPCR) comparing dwarfing (M27, M9) and vigorous (M793) rootstocks, carbohydrate analysis	Dwarfing rootstocks exhibited a downregulation of *MdAUX1* and *MdLAX2* auxin transporters, among other differentially expressed genes. Further, starch synthesis was upregulated, and dwarfing rootstocks contained higher starch and lower fructose and glucose.	[47]

AUX1	Apple (*Malus domestica*)	*MdAUX1*: *MDP0000885425* (*M. domestica* genome v1.0)	Hanfu (diploid and autotetraploid seedlings)	Phenotyping, Gene expression (Tag-seq and qPCR) comparing diploids and autotetraploids	Autotetraploid plants exhibited dwarfism. *AUX1* was found to be downregulated, in addition to changes in brassinosteroid gene expression (see below).	[45]
AUX1/ LAX family	All plants (focus on models)	*AUX1/LAX* genes across species		Review	Auxin transport, via AUX1/LAX proteins, PINs, and PGP/ABCBs, plays a major role in many architecture-related developmental processes, such as root development (primary and lateral root, gravitropism, root hairs), phyllotactic patterning, leaf morphogenesis, and inflorescence architecture.	[59]
IGT						
TAC1	*Prunus persica*	*PpeTAC1*: *Ppa010082* (*P. persica* genome v1.0) *AtTAC1*: *At2g46640* (TAIR10)	Crimson Rocket	Pnome to map pillar mutation, gene expression, branch and flower bud angle phenotypes, *AtTAC1* overexpression in Arabidopsis	Pillar peach variety "Crimson Rocket" has insertion within *PpeTAC1* gene. Overexpression of *AtTAC1* in Arabidopsis leads to narrow branch angles. *PpeTAC1* and *AtTAC1* are expressed in branch tips.	[42]
TAC1, LAZY1, LAZY2	Apple (*Malus domestica*)	*MdoTAC1a*: *MG837476* *MdoTAC1b*: *MG837477* MdoLAZY1: MG837478 *MdoLAZY2*: *MG837479* (Genbank)	Rootstock: *Malus robusta* Scion: McIntosh, Wijcik, Granny Smith, Fukushima spur	Gene expression (qPCR) comparing cultivars representative of four architectural ideotypes.	Comparison of *IGT* gene expression between McIntosh (standard), Fukushima spur (spur), Granny Smith (tip-bearing), and Wijcik (columnar), showed decreasing levels of *TAC1* in shoot tips in that cultivar order, with the lowest expression of all identified *IGT* genes in the columnar cultivar in all tissues.	[55]

DRO1	Apple (*Malus domestica*)	*MdDRO1*: *MDP0000142588* *MdDRO2*: *MDP0000151294* *MdDRO3*: *MDP0000723826* *MdPIN11*: *MDP0000125862* (*M. domestica* genome v1.0)	Rootstock: M9, Baleng Crab and interspecific hybrids from M9 x BC cross (rooted cuttings)	Root angle phenotyping, gene expression (qPCR in roots tissue), IAA quantification	Deep-rooted Baleng Crab had steeper root angles, and greater root length than M9. M9 showed lower IAA content, higher IAA oxidase activity, fewer amyloplasts, and lower expression of *MdDRO1* and *MdPIN11* architecture-associated genes.	[50]
	Plum (*Prunus domestica*), Peach (*Prunus persica*), Arabidopsis	*PpeDRO1*: *Ppa021925* (*P. persica* genome v1.0) *AtDRO1*: *At1g72490* *AtDRO2*: *At1g19115* *AtDRO3*: *At1g17400* (TAIR10)	Plum seedlings: Stanley Arabidopsis: Columbia	Gene expression (qPCR, GUS), root angle phenotyping, root gravitropism, *DRO1* overexpression in plum and Arabidopsis	*DRO1* and *DRO2* are expressed in roots in Arabidopsis and peach. atdro1 mutants had wider lateral root angles, but no different in primary root gravitropism. *AtDRO1* OE Arabidopsis had narrower lateral root branch angles, distinct upward leaf curling, shorter siliques, narrower shoot branch angle. *PpeDRO1* OE plum roots were longer with greater root/shoot weight than controls.	[49]
IGT Family	Across kingdom	*IGT* gene across species		Review of *IGT* gene studies from the 1930's to the present, phylogenetic analysis	*IGT* genes influence growth angle/gravitropic set point angle of both shoots and roots, which affects access to water and nutrients, density of plantings, structural integrity and soil anchorage, and overall crop productivity.	[34]
GID1						

GID1c	Peach (*Prunus persica*)	*PpeGID1c*: *Ppa018174* (*P. persica* genome v1.0)	Brachytic dwarf (BD), Standard, and a mapping population from a BD x Std cross	Pnome to map *dw* mutation, phenotyping and GA application response, RNAi silencing of *GID1c* in plum, gene expression (qPCR)	BD peaches exhibit extreme dwarfism, primarily attributed to reduced internode length. The *dw* mutation in BD peaches was mapped to *PpeGID1c*. BD peaches showed insensitivity to GA treatment. Silencing *GID1c* in plums led to a BD-like dwarfed phenotype.	[44]
			FenHuaShouXing Tao (FHSXT), QiuMiHong (QMH)	Phenotyping of dwarf (FHSXT) and Standard (QMH) cultivars, GA response and quantification, gene expression (qPCR), yeast-2-hybrid, protein quantification (western)	FHSXT exhibited extreme dwarfism, short internodes, shorter cell length, fewer branches, and longer leaves. FHSXT had high levels of GA and were GA insensitive. *GID1c* was upregulated in FHSXT, as were multiple GA biosynthesis genes (see below). The mutation in FHSXT *GID1c* abolished interaction with DELLA1 in a yeast-2-hybrid assay.	[56]
GID1	Arabidopsis	*AtGID1a*: *At3g05120*, *AtGID1b*: *At3g63010*, *AtGID1c*: *At5g27320* (TAIR10)	Columbia	Phenotyping mutants, gene expression (qPCR), GA treatment and quantification	Double mutants *atgid1a atgid1c* and *atgid1a atgid1b* showed reduced stem height phenotypes, while the triple mutant exhibited severe dwarfing and GA insensitivity. The triple mutant phenotype was partially rescued by loss of function of the DELLA protein AtRGA.	[36]
GA2ox, GA3ox, GA20ox						
GA2ox	Peach (*Prunus persica*)	*PpeGA2ox-1*: *Prupe.1G111900* *PpeGA2ox-2*: *Prupe.1G344000* *PpeGA2ox-3*: *Prupe.3G006700* *PpeGA2ox-4*: *Prupe.4G026300*	QiuMiHong (QMH)	Gene expression (qPCR), PpeGA2ox gene overexpression in tobacco, GA treatment and quantification	Seven *GA2ox* genes were identified in peach and classified into three subgroups, and tissue-specific expression was determined in a standard peach cultivar. Overexpression of	[63]

		PpeGA2ox-5: *Prupe.4G080700* *PpeGA2ox-6*: *Prupe.4G150200* *PpeGA2ox-7*: *Prupe.4G204600* (*P. persica* genome v2.0)			*PpeGA2ox1*, *PpeGA2ox5*, and *PpeGA2ox2* resulted in dwarf phenotypes in tobacco. GA treatment at shoot tips induced expressions of all *PpeGA2ox* genes, but at different rates.	
	Arabidopsis thaliana	*AtGA2ox1*: *At1g78440* *AtGA2ox2*: *At1g30040* *AtGA2ox3*: *At2g34555* *AtGA2ox4*: *At1g47990* *AtGA2ox6*: *At1g02400* *AtGA2ox7*: *At1g50960* *AtGA2ox8*: *At4g21200* (TAIR10)	Columbia-o and *hy5* mutant	Gene expression (GUS reporters, qPCR), *GA2ox* overexpression	Overexpression of *GA2ox* genes inhibited elongation of the hypocotyl, rescued the long-hypocotyl phenotype of hy5 mutants. Overexpression of *GA2ox7* and 8 led to extra shortening of the hypocotyl in *hy5* mutants.	[57]
GA20ox	Apple (*Malus domestica*)	*MpGA20ox1A* *MpGA20ox1B* (Noted from *M. pumila*, a previous name for *M. domestica*. Gene IDs unclear)	Rootstock: M25, MM106 Scion: Greensleeves	Gene expression (qPCR), gene silencing, phenotyping, grafting onto invigorating rootstocks, GA quantification	Silencing of *MpGA20ox1A* and *B* led to reduced height, and reduced internode length and number. Application of exogenous GA rescued the dwarfed phenotype. Transgenic dwarfed scions remained dwarfed after grafting onto invigorating rootstocks.	[35]
GA2ox, GA3ox, GA20ox	Peach (*Prunus persica*)		FenHuaShouXing Tao (FHSXT), QiuMiHong (QMH)	See above (*GID1*)	Expression of several *GA2ox*, *GA3ox*, and *GA20ox* GA biosynthesis genes were upregulated in a dwarfed variety (FHSXT), as was *GID1c* (see above).	[56]
WRKY9						

WRKY9	Apple (*Malus domestica*)	*MdWRKY9*: *MDP0000272940* (*M. domestica* genome v1.0)	Dwarfing rootstock: M.9 Pajam 2, M26, GM256, B9 and M.9 T337 Non-dwarfing rootstock: *M. baccata*, *M. robusta*, *M. sieversii*, *M. prunifolia*, *M. zumi*	Gene expression (qPCR), *MdWRKY9* overexpression in apple, subcellular localization, transcriptional inhibition assays, hormone quantification, CHIP-qPCR	*MdWRKY9* was more highly expressed in dwarfing rootstock. Overexpression of *MdWRKY9* in M26 semi-dwarfing rootstock resulted in dwarfed characteristics, and fewer, but longer roots. *MdWRKY9* binds and inhibits expression of the brassinosteroid biosynthetic gene *MdDWF4* (see below)	[54]
EIN2						
EIN2	Rice (*Oryza sativa*)	*OsEIN2*: *LOC_Os07g06130* *OsEIL1*: *LOC_Os03g20790* (MSU Rice Gene Models)	Nipponbare	Computed tomography (CT), mutant analysis, confocal microscopy, ethylene treatment and quantification, gas barrier treatment, GUS assay, ethylene biosensor	Ethylene-insensitive signaling mutants (*osein2* and *oseil1*) were unaffected by and grew deeper into compacted soil. Shoot and root biomass was increased in ethylene-insensitive mutants grown in compacted soil. Ethylene was slow to diffuse through compacted soils and ethylene detection in the root was shown to increase in compacted soil.	[64]
	Arabidopsis thaliana	*AtEIN2*: *At5g03280* (TAIR10)	Columbia	Gene expression (GUS), root architecture phenotyping on differing Boron concentrations, mutant analysis	Ethylene-insensitive mutant *atein2-1* inhibited increased root hair formation and elongation under low-Boron conditions.	[39]

	All species	Ethylene signaling and biosynthesis genes		Review of ethylene effects on root and hypocotyl elongation, root hair formation, apical hook formation, stem growth, biosynthesis pathway, and signaling pathway	Inhibitory effects of ethylene on root growth observed as early as 1901. Plant grown on aerated soils have high ethylene and strong root growth inhibition when treated with ethylene. Ethylene interacts with GA and auxin pathways to regulate root growth, as well as JA and auxin pathways to regulate root hair formation. Ethylene plays a role in inhibiting stem growth, and can also stimulate stem growth in shaded conditions.	[37]
DWF1, DWF4						
DWF1, DWF4	Apple (*Malus domestica*)	*MdDWF1-1*: *MD13G1007700* *MdDWF1-2*: *MD16G1000400* *MdDWF4-1*: *MD02G1149000* *MdDWF4-2*: *MD15G1263900* *MdDWF4-3*: *MD17G1120200* (*M. domestica* GDDH13 genome v1.1)	Rooted seedlings: M.9-T337, Yanfu No. 6 (YF), Nagafu No. 2 (CF), *M. hupehensis* Rootstock: M.9, CF Scion: CF	Phylogeny, synteny analysis, gene expression (qPCR), hormone treatment and quantification	YF trees are spur type and have lower shoot elongation rate, number of internodes, and average internode length relative to CF. *mddwf1-1* and *mddwf1-2* are highly expressed in CF relative to YF. CF/M.9 (dwarf) trees have lower *mddwf4* and *mddwf1* expression relative to CF/CF.	[52]
DWF4	Apple (*Malus domestica*)	*MdDWF4*: *MDP0000498540* (*M. domestica* genome v1.0)	Dwarfing rootstock: M.9 Pajam 2, M26, GM256, B9 and M.9 T337 Non-dwarfing rootstock: *M. baccata*, *M. robusta*, *M. sieversii*, *M. prunifolia*, and *M. zumi*	Gene expression (qPCR), *MdWRKY9* overexpression in apple, subcellular localization, transcriptional inhibition assays, hormone quantification, CHIP-qPCR	Overexpression of *MdWRKY9* in apple resulted in significantly lower expression of *mddwf4* and lower brassinosteroid content. *MdWRKY9* binds and inhibits expression of the brassinosteroid biosynthetic gene *MdDWF4* (see above).	[54]

DWF1, DWF4	Arabidopsis, Tomato	*AtDWF1*: *At3g19820* *AtDWF4*: *At3g50660* (TAIR10)		Review of multiple BR biosynthetic genes, pathways, and mutant phenotypes and chemicals that led to these findings	*dwf* mutants exhibit extreme dwarfism, with additional alteration in leaf and inflorescence development. DWARF1 is a biosynthetic enzyme involved in reducing C24 of BR. DWARF4 is a cytochrome P450 enzyme involved in hydroxylating C22 of BR and represents a rate-limiting step in biosynthesis.	[33]
IPT3						
IPT3	Apple (*Malus domestica*)	*MdPIN1*: Unclear. Degenerate primers designed based on Arabidopsis, lupin, pea, and *Populus* sequences. *MdIPT3*: Unclear. Degenerate primers designed based on *Malus hupehensis*, Arabidopsis, and cabbage sequences.	Rootstock: M9 and MM (*M. x micromalus*) Scion: Red Fuji Interstock: M9	Gene expression (qPCR), hormone quantification, grafting substitution experiments (rootstock substitutions, rootstock bridging, and bark substitutions)	M9 (common dwarfing rootstock) seedlings showed lower *PIN1* and *IPT3* expression, as well as lower auxin and zeatin across different plant tissues, compared with MM seedlings. Grafting combinations including M9 as rootstock or standard interstock similarly frequently had reduced *PIN1* and *IPT3* expression and reduced hormone levels compared with MM grafting combinations. The reduced levels were largely rescued when MM or Red Fuji were introduced as rootstock substitutions, bridged, or bark substitutions.	[40]
	Arabidopsis	*AtIPT3*: *At3g63110* *AtIPT5*: *At5g19040* *AtAHK2*: *At5g35750* *AtAHK3*: *At1g27320* *AtAHK4*: *At2g01830* (TAIR10)	Col-0	Root architecture phenotyping, gene expression (GUS), hormone treatments, overexpression of cytokinin catabolism genes, mutant	Increasing concentrations ot cytokinin led to decreases in lateral root (LR) density. Loss of *IPT3* and other *IPT* (cytokinin biosynthesis) genes resulted in increased LR formation and density. Similarly, loss of *AHK*	[41]

				analysis of biosynthesis genes	cytokinin receptor genes led to increased LR densities.	
MAX1, MAX2, MAX3, MAX4						
MAX1, MAX2, MAX3, MAX4	Apple (*Malus domestica*)	*MdMAX1-1*: *MDP0000130133* *MdMAX1-2*: *MDP0000677258* *MdMAX1-3*: *MDP0000909874* *MdMAX2-1*: *MDP0000466825* *MdMAX3-1*: *MDP0000197409* *MdMAX3-2*: *MDP0000139334* *MdMAX4-1*: *MDP0000227870* *MdMAX4-4*: Unclear (Based on primer sequences, *M. domestica* genome v1.0)	Standards: McIntosh genotypes 21-S, 31-S, and 77-S Columnar apples: Wijcik genotypes 21-C, 31-C, 77-C	Gene expression (qPCR) comparing standard and columnar phenotypes, strigolactone quantification, overexpression of *MdCo31* in tobacco	*MdMAX* gene expression was frequently higher in columnar apple buds and shoots, as was expression of *MdCo31*. Overexpression of *MdCo31* in tobacco resulted in plants with reduced height, internode lengths, and increase leaf thickness and chlorophyll content. Tobacco *MAX3* was increased in these lines, while tobacco *MAX1* was upregulated only in the line with the shortest stature.	[62]
	Peach (*Prunus persica*)	*PpeMAX1*: *Ppa003950m* *PpeMAX2*: *Ppa002017m* *PpeMAX3*: *Ppa017865m* *PpeMAX4*: *Ppa006042m* (*P. persica* genome v1.0)	Rootstock: Lovell, Bailey, Tennessee natural Scion: Redhaven (standard), Harrow Beauty (standard), Bounty (standard), Crimson Rocket (pillar), Sweet-N-Up (upright)	Gene expression (qPCR), hormone quantification between standard, upright, and pillar growth habits	*PpeMAX3* and *PpeMAX4* expression was higher in in stems following pruning. *PpeMAX3* expression and auxin concentrations were greater in the roots of pillar phenotype. *PpeMAX1-4* expression was intermediate between pillar and standard. Expression of *PpeMAX1*, *PpeMAX2*, and *PpeMAX4* in roots were higher in pillar, but not statistically significant.	[43]

MAX1, MAX2	Apple (*Malus spectabilis*, *M. domestica*, and *M. robusta*)	*MsMAX2*: Used primers based on *MdMAX2* (*MD17G1266700*) *MsMAX1*: Used primers based on *MdMAX1* (*MD15G1057600*) (*M. domestica* GDDH13 genome v1.1)	Rootstock: M. robusta Scion: More-Branching (*MB*) mutant and wild type (WT) of *M. spectabilis* cultivar Bly114, *M. domestica* cultivars T337, M26, and Fuji Nagafu2	Morphological and anatomical phenotypes, hormone quantification, gene expression (transcriptome and qPCR)	*MB* mutants had decreased height, increased branch number, and narrower branch angles. *MsMAX1* and *MsMAX2* were upregulated in axillary buds during outgrowth.	[60]

974 **Figures**

975

976 Figure 1

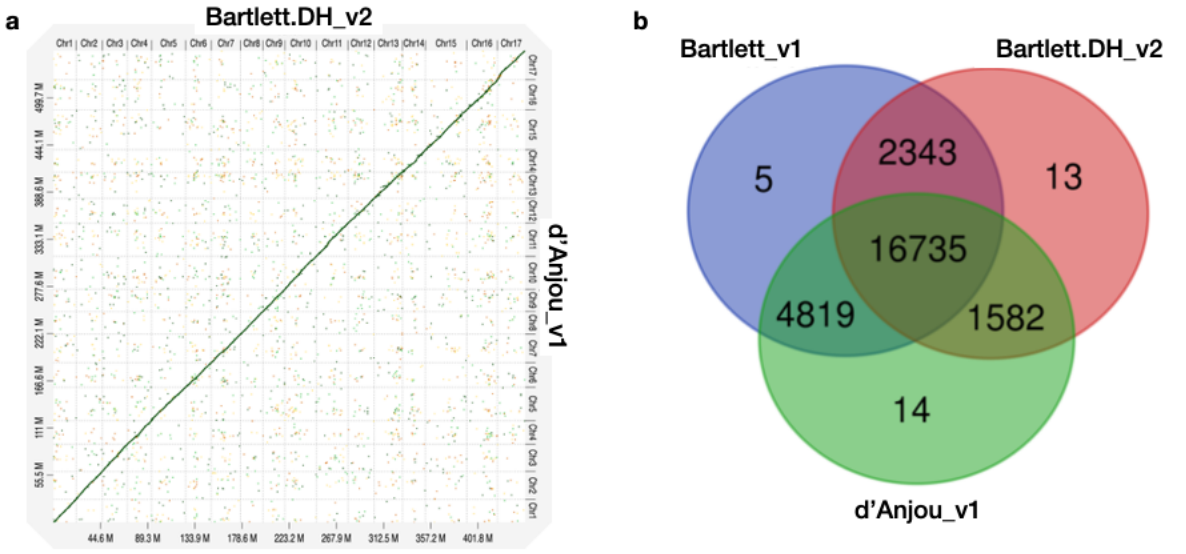

977

978

979 Figure 2

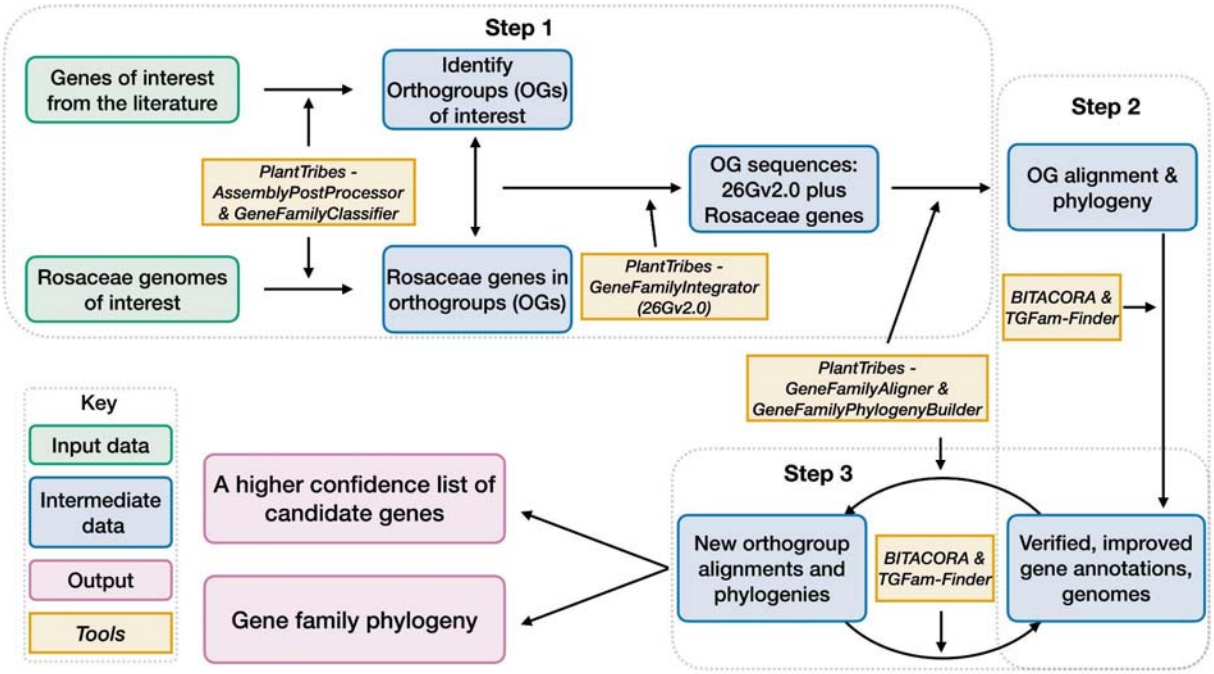

980

981

982

983 Figure 3

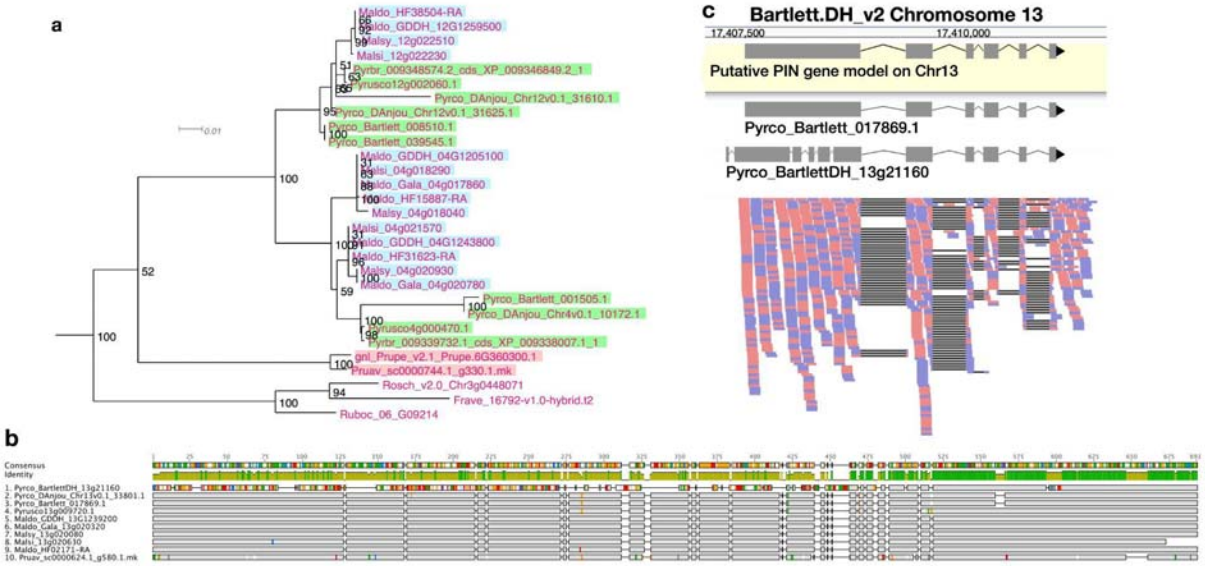

984
985

986 Figure 4

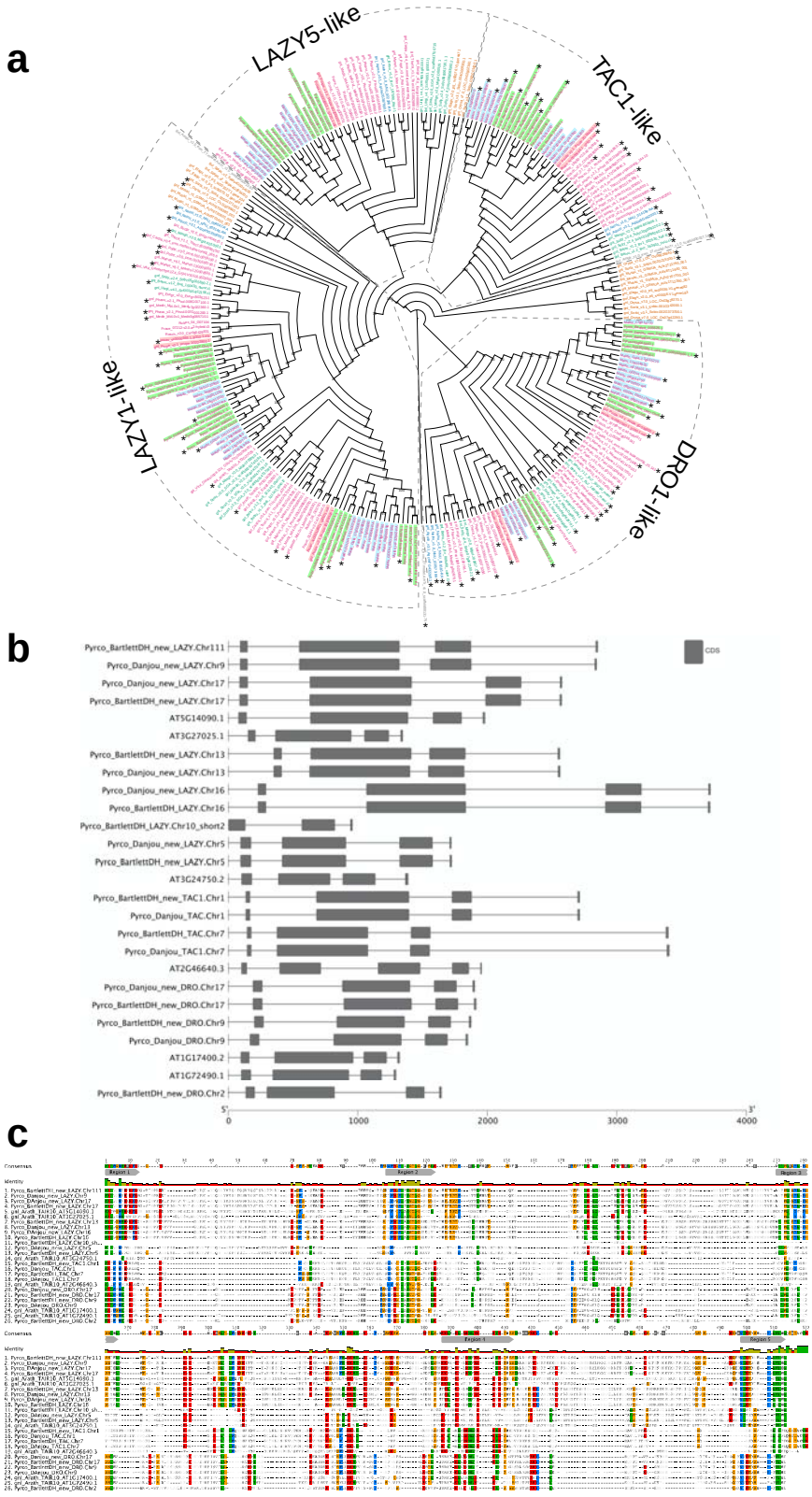

987